
Chapter A.7

The Boreal Climate

Forrest G. Hall · Alan K. Betts · Steve Frolking · Ross Brown · Jing M. Chen · Wenjun Chen
Sven Halldin · Dennis P. Lettenmaier · Joel Schafer

The boreal ecosystem encircles the Earth above about 48° N, covering Alaska, Canada, and Eurasia. It is second in areal extent only to the world's tropical forests and occupies about 21% of the Earth's forested land surface (Whittaker and Likins 1975). Nutrient cycling rates are relatively low in the cold wet boreal soils. Whittaker and Likins (1975) estimate the annual net primary productivity of the boreal forest at $800 \text{ g C m}^{-2} \text{ y}^{-1}$ and its tundra at $140 \text{ g C m}^{-2} \text{ y}^{-1}$, in contrast to tropical forests averaging $2200 \text{ g C m}^{-2} \text{ y}^{-1}$ and temperate forests at $1250 \text{ g C m}^{-2} \text{ y}^{-1}$. However, the relatively low nutrient cycling rates at high latitudes result in relatively high long-term boreal carbon storage rates averaging roughly 30 to $50 \text{ g C m}^{-2} \text{ y}^{-1}$ (Harden et al. 1992), a result of relatively high root turnover from trees, shrubs and mosses with relatively low decomposition rates. Over the past few thousand years, these below-ground storage processes have created a large and potentially mobile reservoir of carbon in the peats and permafrost of the boreal ecosystem. Currently, the boreal ecosystem is estimated to contain approximately 13% of the Earth's carbon, stored in the form of above-ground biomass and 43% of the Earth's carbon stored below-ground in its soils (Schlesinger 1991). Meridional gradients in atmospheric CO_2 concentrations suggest that forests above 40° N sequester as much as 1 to 2 gigatons of carbon annually (Denning et al. 1995; Randerson et al. 1997), or nearly 15 to 30% of that injected into the atmosphere each year through fossil fuel combustion and deforestation. Given the enormous areal extent of the ecosystem, roughly 20 Mkm^2 (Sellers et al. 1996b; Fig. A.45), shifts in carbon flux of as little as $50 \text{ g C m}^{-2} \text{ y}^{-1}$ can contribute or remove one gigaton of carbon annually from the atmosphere. The size of the boreal forest, its sensitivity to relatively small climatic variations, its influence on global climate and the global carbon cycle, therefore, make it critically important to better understand and represent boreal ecosystem processes correctly in global models.

In Sect. A.7.1 we will first describe the global boreal ecosystem, its landscape structure and composition and the extant factors that have shaped this landscape; its palaeo- and modern climate, and its fire disturbance history. We will pay particular attention to the effects of high-latitude climate change on snow extent and depth.

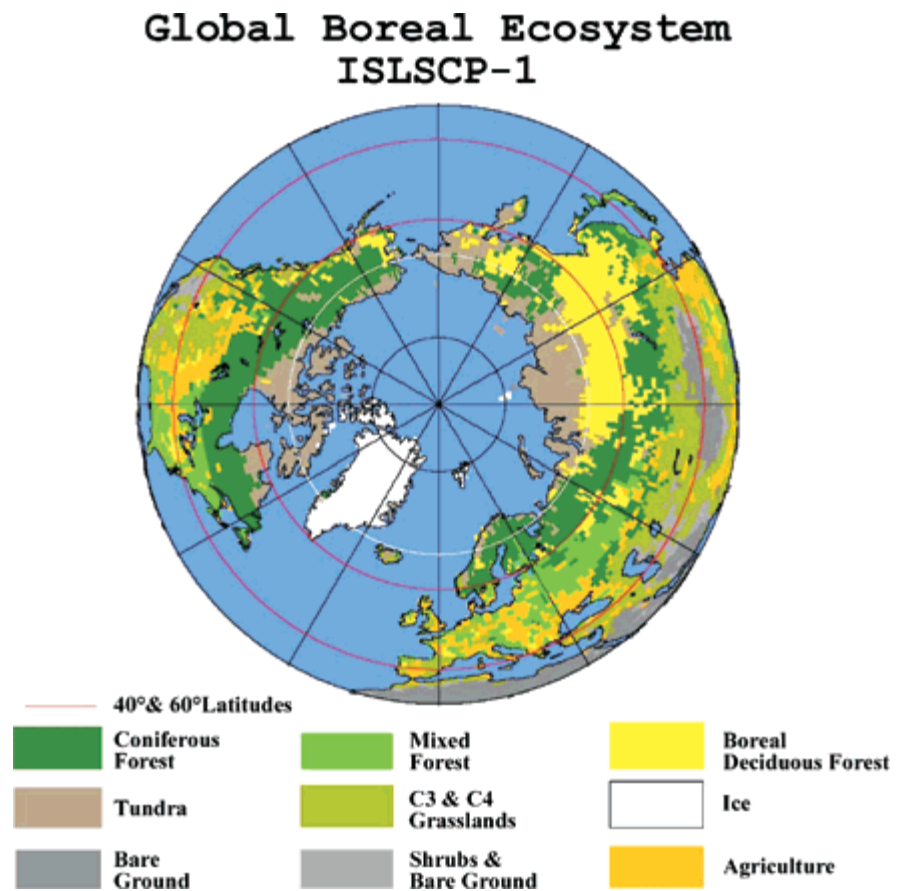
In Sect. A.7.2 we will review research relevant to energy dissipation and transport between the boreal land surface and atmospheric boundary layer. We will discuss how the boreal landscape, its albedo and biophysical control on the surface energy and water budget affects atmospheric circulation in the short term and climate at longer time scales. In Sect. A.7.3 we will consider biogeochemical cycling by the boreal landscape, focusing on carbon uptake and release for both carbon dioxide and methane; how the cycling rates are affected by land-cover type, climate, soils and surface hydrology. Finally, in Sect. A.7.4 we will examine the projected impacts of future climate change on the land surface and potential feedbacks, including the effects of variation in snow cover extent and duration, carbon sequestration and release by the surface to the atmosphere and the effects of land-cover change.

A.7.1 The Boreal Ecosystem, Boreal Climate and High-latitude Climate Change and Variability

The boreal ecosystem, or taiga, has no precise definition beyond the meaning of its name, cold northern ecosystem. By about 7 000 years ago, the great ice fields and glacial lakes that had covered Canada, part of the US and Eurasia during the last glacial maximum, had withdrawn from what now constitutes the boreal ecosystem, leaving behind in their retreat bare rock, sand, gravel and clay. Following that, precursors to modern boreal species recolonised the boreal landscape from their ice-age refuges in mountains and warmer coastal regions, and from the warmer southern regions as far south as 30° N (Larsen 1980). Over time, these soil horizons were overlain by mineral soils from wind erosion, and organic soils and peats as the boreal soils accumulated detritus from forests and mosses. Harden et al. (1992) place historical carbon accumulation rates in these peat soils in the range of 10 to $50 \text{ g C m}^{-2} \text{ y}^{-1}$.

Topography, frigid long winters, followed by hot dry summers, in combination with frequent large-scale lightning-induced fires are the dominant forces that structure the patchiness and composition of the vast majority of the boreal landscape. For a majority of the boreal

Fig. A.45.
Polar boreal vegetation map at 1° spatial resolution derived from ISLSCP I (Sellers et al. 1996b) land-cover dataset based on AVHRR data (DeFries and Townshend 1994). White latitude line is Arctic Circle; red latitude lines drawn at 60 and 40° N



ecosystem, its species have limited commercial value and deforestation from logging is small. Where logging is of economic importance and fire is controlled, such as in the north-European boreal forests of Sweden and Finland, patchiness is largely determined by property boundaries.

These conditions have selected for a few dominant species, including stands of spruce, tamarack, fir and pine as well as aspen, birch and poplar. The ecosystem is also populated by vast wetland complexes (Tarnocai et al. 2000) consisting of lakes, bogs, fens, marshes, swamps and muskeg. For the purposes of this chapter, we will consider the boreal ecosystem to consist of the sub-arctic forests (predominantly coniferous) and wetlands (muskeg) lying primarily above 48° N as well as the tundra, primarily above about 60° N and below the Arctic Circle. Above roughly 60° N, the forest degrades gradually to forest shrubland, then tundra. The southern limit is less clearly defined, transitioning gradually into prairies and croplands, and more temperate deciduous and coniferous forests and grasslands.

To understand the first order interactions between the atmosphere and land, boreal vegetation types can be lumped into the broad categories shown in Fig. A.45, which indicates that coniferous, deciduous and mixed

coniferous/deciduous boreal forests occupy roughly 20 Mkm² between 60 and 40° N. It is within these latitudes that tracer model studies indicate forests may be a strong sink for carbon dioxide of approximately 1 to 2 gigatons annually (Denning et al. 1995; Randerson et al. 1997).

These wetlands are generally unresolvable from either AVHRR or Landsat Thematic Mapper data (Hall et al. 1997; Beaubien et al. 1999), although ground survey maps do exist (Tarnocai et al. 2000). As will be seen in Sect. A.7.3.5, wetlands play an important role in methane flux to the atmosphere and thus the future development of a remote sensing capability to estimate their areal extent and type (fen, marsh, bog or swamp) is important.

A.7.1.1 Climate and Boreal Vegetation

Larsen (1980) observes of the boreal forest, "It is bounded on the north over most of Canada and Eurasia approximately by the position of the July 13 °C isotherm with marked departures in regions possessing montane or oceanic climatic influences. The southern limit of the boreal region in central and eastern Canada is bounded roughly by the position of the July 18 °C isotherm. But

where drier conditions prevail, the southern edge of the forest border lies to the north of this isotherm, trending into regions where annual precipitation is greater. The same general relationships between the boreal forest and summer isotherms hold also in Eurasia.” The harsher climate at the northern transition zone, accompanied by lower soil temperatures, results in an open wooded lichen landscape, which slowly merges into the tundra.

The boreal ecosystem so defined, consists of three major climatic zones: largely flat continental interiors, montane and coastal regions, including the Pacific coast, Hudson Bay, and the Arctic coast in Eurasia and the East Siberian seas. The climate of Scandinavia is maritime to the west and gradually shifts over to continental in the eastern parts of Finland. The climate in the North American boreal zone is typified by short, warm, moist summers and long, cold, dry winters. Mean annual temperatures range from -10 to -4.5 °C in the interior Yukon and Alaska, 1 to 5.5 °C in northern coastal British Columbia and -4 to 5.5 °C in the extensive boreal shield ecozone (Ecological Stratification Working Group (ESWG) 1996). The northern continental plain of the boreal forest retains ground snow cover for up to eight months in a year resulting in a short growing season, in comparison with the Avalon peninsula which experiences milder, wetter weather due to the buffering effect of the Atlantic ocean (ESWG 1996). The North American boreal forest region is characterised by large, often monotypic stands of white and black spruce, jackpine, balsam fir, and tamarack. Historically, this predominantly coniferous forest had a minor component of trembling aspen and balsam poplar (Rowe 1972). An increase in the black spruce and tamarack species component occurs as the tree line is approached (ESWG 1996). From north to south, the southern transition zone in the west incorporates an increasing amount of trembling aspen, balsam poplar, and willow. The transition to steppe-like vegetation is made across a positive 2 °C mean temperature gradient (Singh and Wheaton 1991). In the east, the southern transition zone is characterised by intermingled temperate species of eastern white and red pine, yellow birch, sugar maple, and black ash (Rowe 1972). The appearance, structure and function of the boreal forest is remarkably similar at all longitudes, consisting primarily of needleleaf evergreen and needleleaf deciduous conifer, underlain by low shrubs and herbaceous plants, atop a thick layer of mosses and lichens. From the functional viewpoint of energy balance and biogeochemical cycling, the most important aspect of species variation within the boreal ecosystem is the variation in structural characteristics from one species to the next, i.e. deciduous versus evergreen and broad versus needleleaf.

In addition to climate change, fire and insect, defoliation plays a dominant role in shaping boreal forest landscapes (Suffling 1995; Hogg 1999), see Sect. A.7.1.2.

A.7.1.2 Effects of Fire and Insects on Vegetation and Land Cover

Fire is a central part of the life cycle of boreal ecosystems except where logging is of economic importance and fire is controlled in areas such as Northern Europe, for example. Although fires burn the boreal forest regularly, new trees quickly emerge in most burnt areas. The history of Canada’s boreal forest has been mostly cycles of destruction and renewal by wild fires. Lightning caused 35% of Canada’s forest fires since 1930 but was disproportionately responsible for 85% of the burned area. Most fires were small, with 2–3% of the fires growing to more than 200 ha and eventually contributing to $\sim 98\%$ of the total burned area (Weber and Flannigan 1997). The fire season in Canada ranges from April through October. Typically, there is virtually no winter activity but a flurry of spring fires after snow melt, followed by a decline as green-up progresses northward. Lightning-induced fires are most active in mid-summer and cease in the autumn.

As shown in Fig. A.46, the period of 1930–1979 saw relatively low forest fire activity in Canada, with the total burned area of 1.1 Mha y^{-1} on average and a range from 0.2 to 3.8 Mha y^{-1} (Weber and Flannigan 1997). During the last two decades since 1980, the average total burned area increased to 2.6 Mha y^{-1} , with a maximum 7.6 Mha y^{-1} in 1989. Another high fire activity period occurred during the period 1850–1920, with mean burned area of ~ 2.6 Mha y^{-1} as inferred by Chen et al. (2000) based on their analyses of forest age structure information from 1920 (Kurz et al. 1995). While the high fire activity period in the recent decades might be related to climate change, the large fire disturbance rates in late 19th century and early 20th century were probably induced by human settlement.

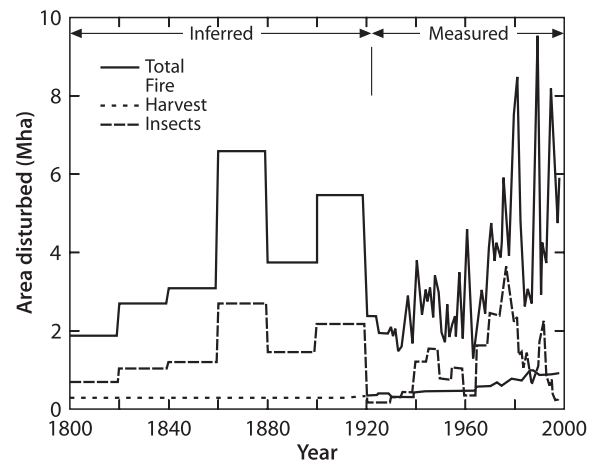


Fig. A.46. Measured and inferred areal extent of disturbance in Canada’s forests since 1800 (after Chen et al. 2000). Forest age structure data for 1920 (Kurz et al. 1995) were used to infered disturbed areas before 1920

In addition to forest fire, insect-induced mortality and harvest affect the carbon cycle of forest ecosystems. The total disturbed area was large during 1860–1920 and 1980–1998, and small during the other periods in the 19th and 20th century (Weber and Flannigan 1997; Kurz et al. 1995; Canadian National Forestry Database Program, <http://www.nrcan.gc.ca/cfs>; Chen et al. 2000).

This temporal distribution of disturbance rates resulted in significant variations in the percentages of young and less productive stands (i.e. < 20 years old), productive stands (i.e. 20–100 years old), and old and less productive stands (i.e. > 100 years old). From 1800–1820, fire and insect-induced mortality rates were lower than their pre-industrial averages. Consequently, the percentage of young stands decreased while that of productive stands increased. The increasing disturbance rates from 1820 to 1880 reduced the percentage of productive stands to a minimum of 41% around 1880. The decreasing trends in the percentage of productive stands has reversed since then and reached a maximum of 71% in 1940, as fire and insect-induced mortality rates decreased in this period. From 1940–1970, the fire and insect-induced mortality rates were still low, but the stands disturbed during the 1860–1920 period entered into old and less productive ages, reducing the percentage of productive stands. The increases in fire and insect-induced mortality rates during the last two decades increased the percentage of young stands substantially and reduced the percentage of productive stands further.

A.7.1.3 High-latitude Climate Change

At the present rate of increase, atmospheric CO₂ concentration will double before the end of the next century (Houghton et al. 1995). Sensitivity experiments made with AGCMs point to large temperature increases in the northern high latitude continental interiors (Schlesinger and Mitchell 1987; Houghton et al. 1995; Sellers et al. 1996a), partly due to projected changes in the polar sea ice climatology and snow-albedo feedbacks. A significant surface warming trend was observed in the boreal zone during the 1980s and early 1990s, reaching 1.25 °C per decade within the Canadian interior (Chapman and Walsh 1993). Serreze et al. (2000) estimated that approximately half the pronounced recent rise in surface Northern Hemisphere temperatures reflected changes in atmospheric circulation. Thompson and Wallace (1998) demonstrated that the predominantly positive phase of the Arctic Oscillation over the last three decades of the 20th century had a major role in the recent warming observed over Eurasia. Correlation of the Thompson and Wallace Arctic Oscillation index with Northern Hemisphere monthly snow cover extent over the 1972 to 2000 period revealed statistically significant correlations over

the January–March period, with a maximum correlation in March (–0.583). Further analysis by sub-regions revealed that this link was concentrated over western Eurasia with no significant associations over North America. Dai et al. (1997) have determined that since 1900 zonal precipitation is increasing at all latitudes, but especially above 40° N. Within the troposphere, the arctic atmosphere has retained nearly the same temperatures since at least the late 1970s (Chase et al. 2002), which is consistent with regional surface changes being due to circulation pattern changes, rather than a uniform tropospheric warming. Arctic sea ice trends (Pielke et al. 2000; <http://faldo.atmos.uiuc.edu/CT>) also document a more complex pattern of temporal variability, with total arctic 2002 sea ice areal coverage returning to near the extent observed at the beginning of the satellite record in the early 1980s.

A.7.1.4 Changes in Snow Extent, Depth and Duration

Although the available data have a number of uncertainties and shortcomings for documenting snow cover variability and trends over the Northern Hemisphere boreal forest zone, they provide evidence that this region has experienced a significant reduction in spring snowpack over the second half of the 20th century. The reduction is in response to enhanced spring warming over Northern Hemisphere high latitudes (Fig. A.47). There are some indications that winter snow depths have increased over northern Eurasia (Ye et al. 1998) which is consistent with observed trends of increased precipitation. However, further analysis of *in situ* snow depth and snow cover extent data, particularly the updated Soviet snow-depth dataset, is required to confirm the continuation of this trend. Winter snow depths decreased over much

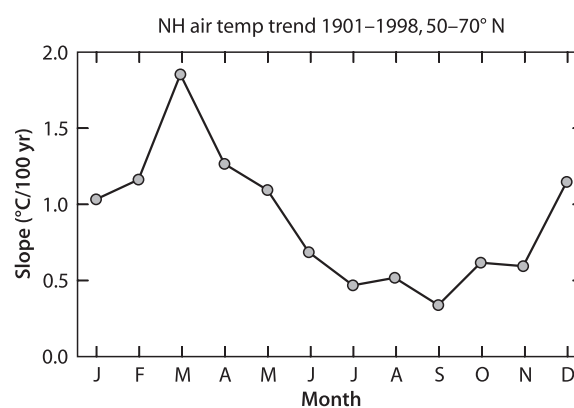


Fig. A.47. Linear trend in Northern Hemisphere land temperatures averaged over 50–70° N for the 1901–1998 period. Computed using an updated version of the Jones (1994) gridded land-surface air temperature anomaly dataset. Trends are statistically significant for the February–September period

of Canada in the mid-1970s in response to a change in atmospheric circulation (Brown and Braaten 1998).

Trends of snow cover extent (1972–1998) from satellite data show significant reductions in spring snow cover over high-latitude and mountainous regions of the Northern Hemisphere, but less change over the boreal forest zones of North America and central Eurasia. A recent climate modelling study by Fyfe and Flato (1999) reported a clear elevational dependency in simulated temperature warming linked to the rise in the snow line and amplified warming from the snow-albedo feedback. It is speculated that the lagged response over the boreal zone is related to the deeper snowpack in these areas, and to the reduced snow cover-albedo feedback over forest.

While there is a clear negative correlation between Northern Hemisphere temperatures and snow cover extent (Robinson and Dewey 1990), surface snow cover conditions represent an integrated response to temperature and precipitation. Thus, atmospheric circulation plays an important role in snow cover variability and change. Dominant modes of atmospheric circulation such as the Pacific-North America (PNA) and North Atlantic Oscillation (NAO) have been shown to exert strong influences on North America and Eurasian winter snow cover respectively.

A.7.1.4.1 Changes in Snow Extent

The National Oceanic and Atmospheric Administration's (NOAA) weekly snow cover dataset provides the longest record of *hemispheric-wide* snow cover extent and has been used extensively to monitor trends in snow cover extent (e.g. Robinson et al. 1993) and to investigate snow cover-climate relationships (e.g. Gutzler and Rosen 1992; Karl et al. 1993; Groisman et al. 1994). The data consist of digitised weekly charts of snow cover derived from visual interpretation of NOAA visible satellite imagery by trained meteorologists. The charts were digitised on an 89×89 polar stereographic grid for the Northern Hemisphere with a 190.5-km resolution at 60° N. Regular monitoring of Northern Hemisphere snow cover with visible satellite imagery began in November 1966 (Dewey and Heim 1982), but the sub-point resolution of the pre-1972 satellites was ~ 4.0 km compared to 1.0 km for the VHRR launched in 1972 (Robinson et al. 1993). Pre-1972 data have recently been re-charted at Rutgers University to extend the NOAA weekly dataset back to 1966. These data were unavailable at the time this chapter was being prepared.

NOAA weekly snow data from 1972–1998 were used to investigate snow cover trends over the boreal forest region of the Northern Hemisphere. This was a period of widespread warming with significant warming trends in most months of the year over the Northern Hemisphere

boreal zone (Fig. A.47). This warming was accompanied by significant reductions in Northern Hemisphere snow cover extent over the May to August period (Fig. A.48).

To characterize the spatial and temporal characteristics of snow cover changes over this period, regression analysis was carried out at each NOAA gridpoint of the number of days with snow cover in the first and second halves of the snow year.

The results (Fig. A.49 and Fig. A.50) show evidence of a marked seasonal difference in snow cover trends, with snow cover increases in the autumn half of the snow season, and widespread snow cover reductions in the spring over many areas of the Northern Hemisphere.

The trend toward reduced spring snow cover is consistent with the spring snow cover feedback mechanism observed by Groisman et al. (1994), i.e. decreased snow cover reduces surface albedo, increases surface absorption of radiation, raises surface temperatures, and hence increases snow melt. The areas experiencing the largest significant reductions in spring snow cover were western mountain regions of North America (particularly the Pacific NW), the Canadian Arctic Islands and Ungava peninsula, the Central Siberian Plateau and Yablonovyy Range, and a broad swath running from the Caucasus Mountains to Tibet. Over these areas spring snow cover reductions were of the order of 1.0 d yr^{-1} . The boreal forest region of NA, heavily forested by evergreen conifers, showed relatively little change in spring snow cover perhaps because the snow cover feedback is weak, due to strong shadowing by the evergreen conifers which reduces markedly the difference between snow-on and snow-off albedo. In Eurasia, where deciduous conifer is abundant, snow-on versus snow-off albedos differ significantly and most of this region experienced spring snow cover reductions (with the exception of the area between 40 and 80° E where spring snow cover increased slightly).

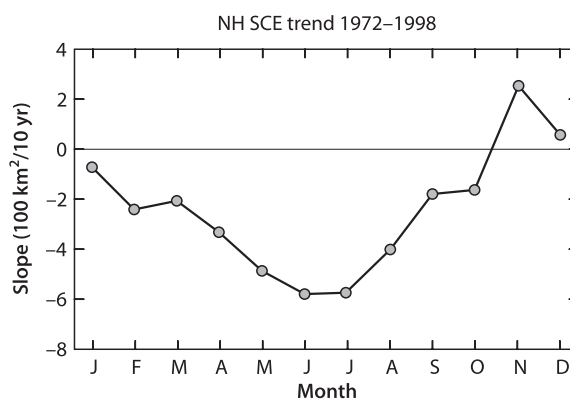


Fig. A.48. Trends in Northern Hemisphere snow cover extent from 1972–1998 from NOAA weekly data. Reductions in the May–August period are statistically significant

Fig. A.49. Contoured values of the slope t -statistic for change in snow cover duration in the first half of the snow year (August–January) over the 1972–1998 period. Values greater than ± 2 indicate locally significant trends

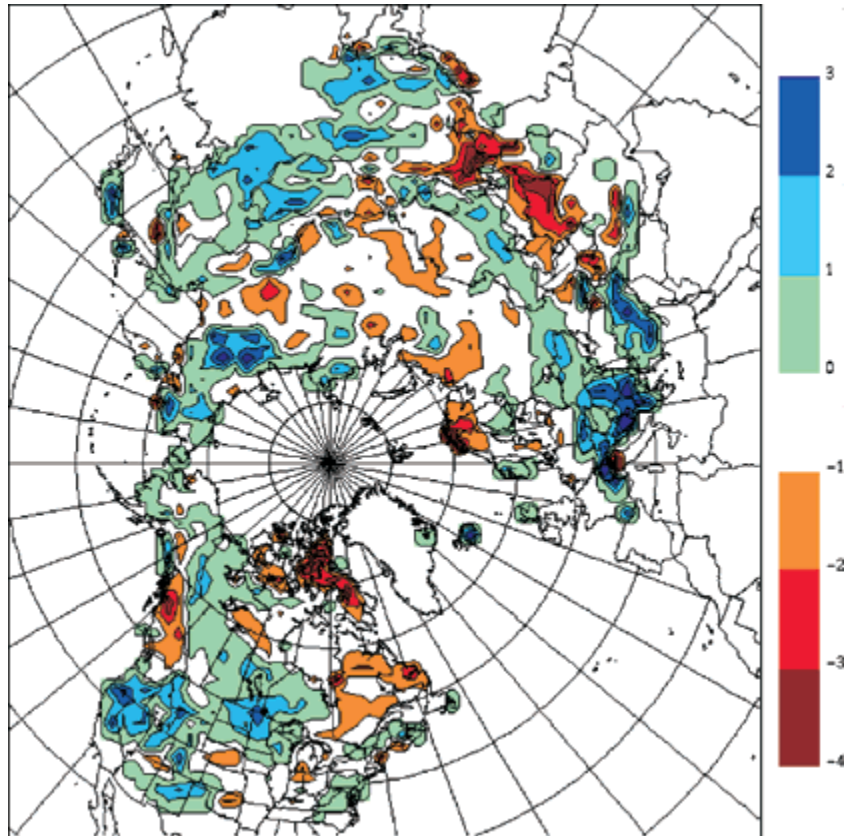
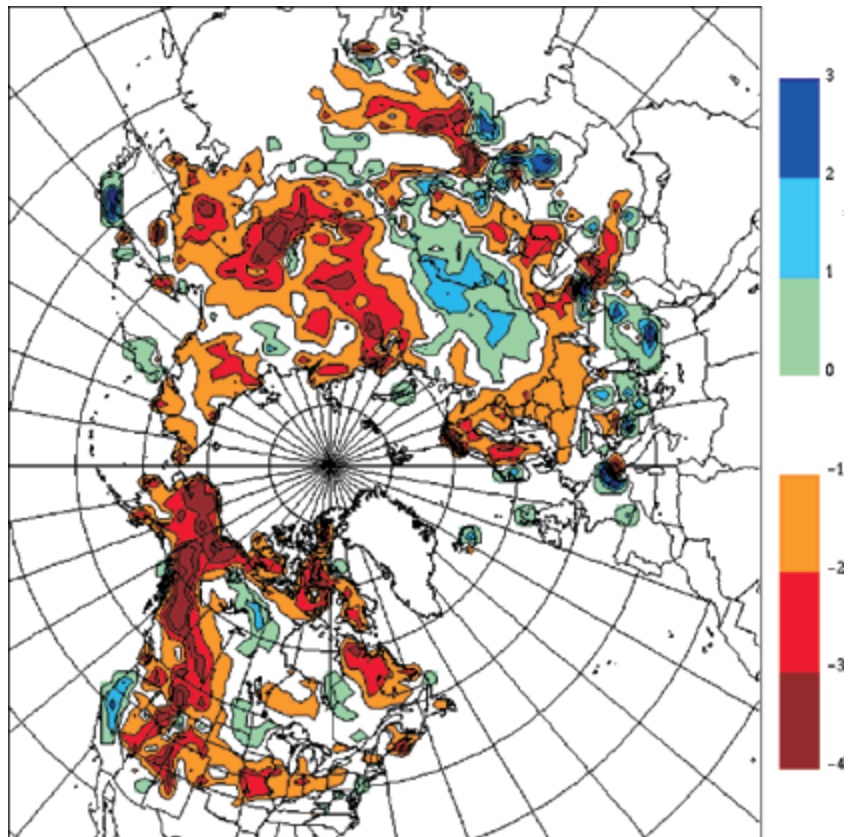


Fig. A.50. Contoured values of the slope t -statistic for snow cover duration in the second half of the snow year (February to July) over the 1972–1998 period. Values greater than ± 2 indicate locally significant trends



A.7.1.4.2 Trends in Snow Depth and Duration

In situ observations of daily snow depth, which provide the longest record of snow cover depth over individual plots, can be used to investigate satellite snow cover trends, and to extend the satellite snow cover record back in time. These data also provide information on the timing and duration of the snow cover season. The two countries with the largest fraction of the Northern Hemisphere boreal forest zone, Canada and Russia, have historical snow depth data going back to the early 1900s. However, the observation programmes and the spatial and temporal distributions of the data are quite different with respect to monitoring snow cover in the boreal forest. Both countries also have *in situ* snow water equivalent observations from snow courses, but these do not cover extended periods and are less suitable for investigating long-term snow cover variability.

Canadian snow depth observations are made by ruler at open locations (often airports) and may not be fully representative of snow conditions in forested areas. This contrasts with snow depth measurements in the Former Soviet Union which were made from snow stakes located to represent the area surrounding a climate station. A description of Canadian snow depth data is provided by Brown and Braaten (1998) and the data are available on CD-ROM (MSC 2000). A CD-ROM compilation of Former Soviet Union historical snow depth data for the period 1881–1995 is provided by the US National Snow and Ice Data Service (NSIDC 1999).

There are few long-term daily snow depth observations in Canada north of $\sim 55^\circ$ N before World War II. Analysis of trends in Canadian snow depth data over the 1946–1995 period (Brown and Braaten 1998) revealed widespread decreases in late winter and early spring snow depths over much of Canada, with the greatest depth decreases occurring in February and March (Fig. A.51). This decrease was associated with significant decreases in spring and summer snow cover duration over most of western Canada and the Arctic (Fig. A.52). Increases are shown as cross-hatched contour lines and decreases as regular lines. The filled squares show the locations of the stations included in the analysis (which were required to have at least 40 years of data in the period). Dark shading is used to highlight areas where changes in snow depth were locally significant ($p < 0.05$). Light shading is used to highlight areas where stations exhibited marginally significant ($0.05 < p < 0.10$) snow depth changes (Brown and Braaten 1998). The snow depth changes were characterised by a rather abrupt transition to lower snow depths in the mid-1970s that coincided with a well-documented shift in atmospheric circulation in the Pacific-North America sector of the Northern Hemisphere that had widespread ecological impacts (Ebbesmeyer et al. 1991).

An indication of longer-term variability in spring snow cover over the southern boreal forest zone of North America can be inferred from reconstructed information on April snow cover extent (Brown 2000). Analysis of NOAA weekly snow cover information showed that during April, snow cover variability is concentrated over

Fig. A.51.
Average change in March mean monthly snow depth over the 1946–95 period (cm y^{-1}) (Brown and Braaten 1998)

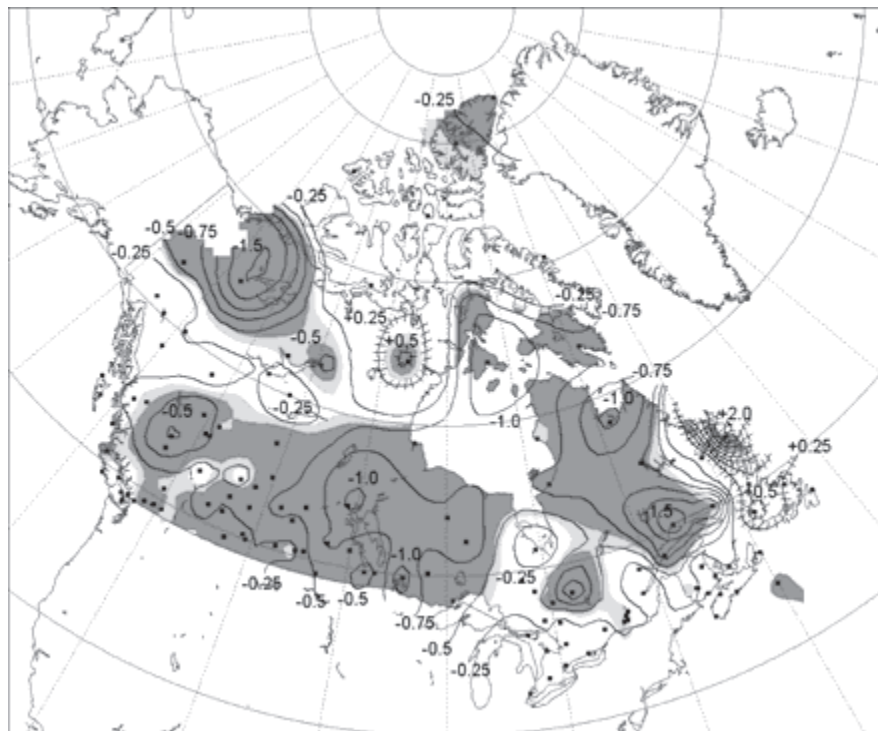


Fig. A.52. Average change in spring (MAM) snow cover duration over the 1946–95 period (d y^{-1}). Shading same as previous figure (Brown and Braaten 1998)

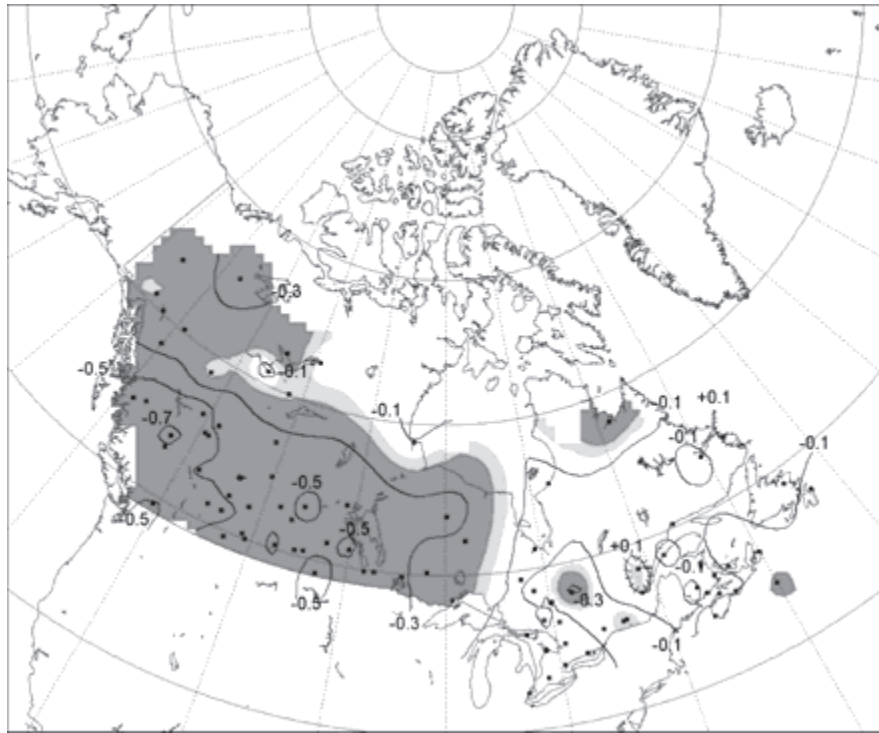
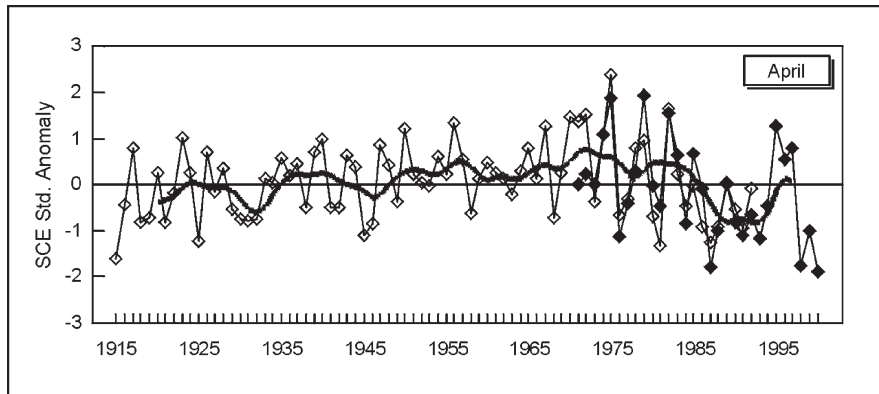


Fig. A.53. Interannual variability in north American monthly snow cover extent for April. *Open diamonds* are anomalies for the station-derived snow cover index; *solid diamonds* are snow cover extent anomalies from the NOAA satellite data; and the *heavy solid lines* are the result of passing a 9-year binomial filter to the combined station (1915–1971) and satellite (1972–2000) anomaly series. Anomalies were standardised with respect to a common 1972–1992 reference period (updated from Brown 2000)



a relatively narrow band from 50–60° N that covers the southern limits of the boreal forest zone. Figure A.53 suggests that reduction in North America spring snow cover is a relatively recent phenomenon, and that snow cover exhibited a gradual increase from the early 1900s to the early 1970s. However, analysis of area-averaged snow depth information for April showed evidence of a significant decreasing trend that began ~1945. Mean snow depths were estimated to have approximately halved over the 1945–1997 period. These results suggest that major changes have likely occurred in spring snowpack conditions in the North American boreal zone over the last five decades. The difference between the snow cover extent and depth results can be explained by the relatively deep spring snowpack in the boreal forest regions (i.e. depth changes have little impact on snow cov-

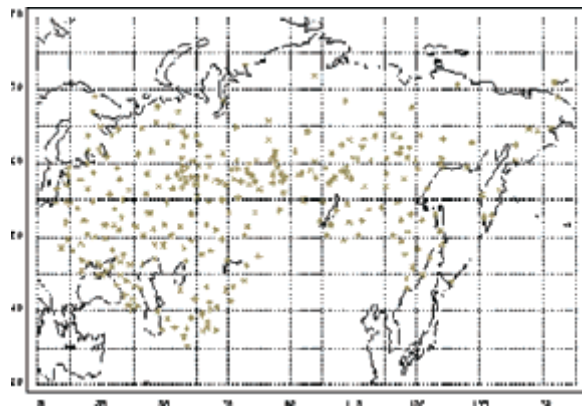
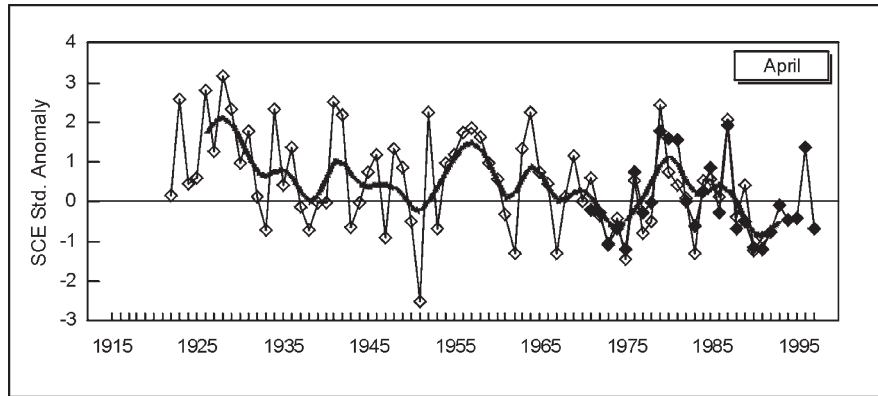


Fig. A.54. Spatial distribution of observing sites in the Historical Soviet Daily Snow Depth dataset (see NSIDC 1999)

Fig. A.55. Reconstructed variation in Eurasian snow cover extent for April (from Brown 2000). Lines and symbols follow the explanation given in Fig. A.53



ered area), and a reduced albedo feedback (Betts and Ball 1997). According to Harding and Pomeroy (1996), the reduced radiation received at the forest floor plus the shelter from vigorous turbulent exchanges act to suppress snowmelt and sublimation. One mechanism explaining the observed decrease in spring snow depths is a reduction in the solid fraction of precipitation accompanying spring warming. Zhang et al. (2000) show that western and central regions of Canada have experienced significant spring (MAM) decreases in the solid fraction of precipitation over the 1950–1994 period (the only season to exhibit this trend).

Figure A.54 shows the spatial distribution of snow depth observed in the Former Soviet Union dataset. Analysis of the first release of the dataset (up to 1984) by Ye et al. (1998) concluded that winter snow depth had increased over most of northern Russia (60–70° N – the boreal forest zone), and had decreased over southern

Russia. The rate of increase over northern Russia was estimated to be 4.7% per decade, which is consistent with estimates of precipitation increases over northern mid-latitudes (Bradley et al. 1987; Vinnikov et al. 1990). The Former Soviet Union snow depth dataset was recently extended to 1995. Reconstruction of snow cover extent over Eurasia by Brown (2000) showed evidence of a significant reduction in April snow cover over the 1922–1997 period (Fig. A.55). During April, the snow line is usually located just to the south of the Eurasian boreal forest zone. Brown (2000) determined that increasing winter season snow depth and reduced spring snow cover extent were consistent with concurrent trends of warming and increased precipitation.

A.7.2 Energy Dissipation and Transport by the Boreal Landscape

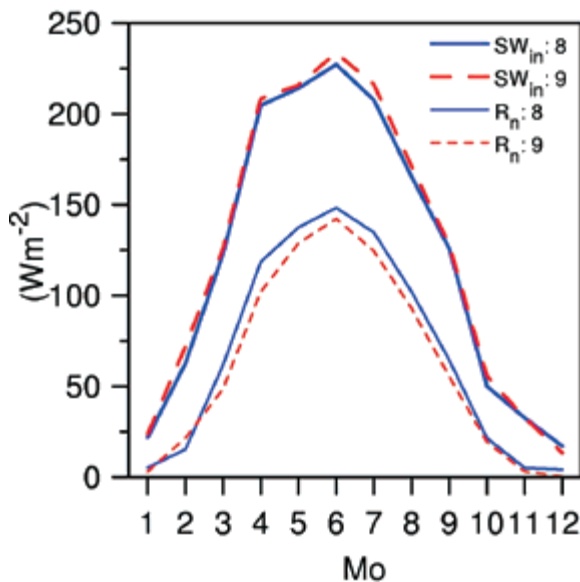


Fig. A.56. Annual cycle of incoming short wave and net radiation (1: January)

The amount of solar energy reaching the land surface during the day varies seasonally and is determined by daylength, solar elevation, cloud cover and atmospheric opacity. The fraction of the sun’s incident energy absorbed by the land surface is in turn determined by surface reflectivity (albedo). The manner in which the surface partitions the absorbed energy into sensible and latent heat is a major determinant of boundary layer dynamics, weather and climate patterns (see Fig. A.3). The partitioning of the net radiation into the sensible and latent heat fluxes and ground heat flux is controlled by the availability of water for evaporation (which is dramatically affected by the seasonal cycle of soil freezing), and by the biophysical controls on transpiration in the warmer months.

Figure A.56 shows the annual cycle of incoming short-wave radiation (SW_{in}) and net radiation (R_n) at the surface for two BOREAS (Boreal Ecosystem-Atmosphere Study) mesonet sites (Thompson, site #8 and the old jackpine, site #9) in the BOREAS northern study area (from Betts et al. 2001). The variation in the net radiation seasonal cycle is very large at this latitude and it

drives the very large seasonal cycle of temperature. There is also a visible and important seasonal asymmetry with respect to the summer solstice in Fig. A.56. In April, both SW_{in} and R_n are considerably larger than in August.

This must be a consequence of lower cloud cover in April, associated with the relative humidity minimum (shown later in Fig. A.58), since the mean solar zenith angle is greater in April than in August.

A.7.2.1 Effect of Soil Type on Surface Energy Partitioning

Figure A.57 shows the three-year (1994–1996) average annual cycle of temperature. The solid lines are mean air temperature at about 6 m above the canopy for Thompson, site #8 and NOJP, site #9. The differences in temperature at this level are very small on the seasonal scale. The dotted and dashed lines, however, labelled with the site numbers, are soil temperatures (at 10 cm and 50 cm depth respectively). Here below ground, the intersite differences are very large. The annual cycle of soil temperature at the jackpine site (with a sandy soil and only a thin lichen ground cover) is much larger than at the mixed spruce site at Thompson, where there is an organic soil with a thick overlying moss layer. At this site, the annual cycle of temperature at 50 cm is small, and the soil at this depth is still frozen in June. This subsurface heterogeneity is an important feature of the landscape and, along with the vegetation type itself, affects surface fluxes since, for example, water is unavailable for transpiration until the ground melts in spring (as we shall see later). However, the sub-surface heterogeneity of temperature is not reflected in the temperature cycle above the canopy.

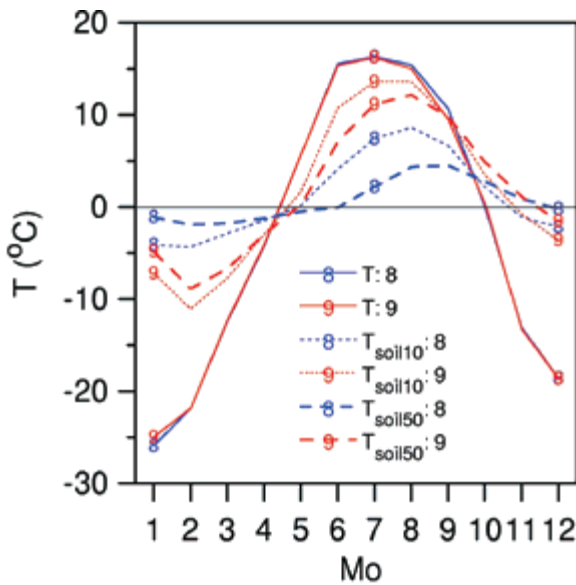


Fig. A.57. Annual cycle of air and soil temperature (1: January)

Figure A.58 shows the annual cycle (1994–1996) of relative humidity above the canopy, showing the remarkable seasonal asymmetry over the boreal forest. In spring (April is month 4) when temperatures are still below freezing but the solar elevation and the net radiation are increasing rapidly, the relative humidity is at a minimum. The minimum day-time relative humidity is very low, often below 25%, as water is generally not available for evaporation at the surface. Evaporation is so low in spring that the forest could be thought of as a “green desert”. Consequently the dry boundary layer in spring can be as much as 2 000 m deep, driven by very large sensible heating with very little evaporation (Betts et al. 1996, 1999, 2001). Throughout the spring, summer and early autumn, mean relative humidity rises to an October peak as the surface becomes warm relative to the atmosphere. In October, the ground has not frozen at either site and water is readily available for evaporation. This seasonal asymmetry in relative humidity is in sharp contrast to the seasonal thermal cycle with a mid-summer maximum, and is an important characteristic of the northern latitudes. The seasonal phase lag of ground temperature with respect to air temperature, which is sharply increased by the phase change of soil water, severely restricts evaporation in spring, when the ground is frozen, while the reverse is true in the autumn, until the ground freezes.

The freezing and thawing of the soil moderates winter temperatures because during the freeze process the effective heat capacity of the soil is increased by a factor of 20 (Viterbo et al. 1999). It introduces a significant lag into the system. In spring a significant part of the net radiation goes into melting the ground, and lakes (and in warming them). This energy becomes available in the

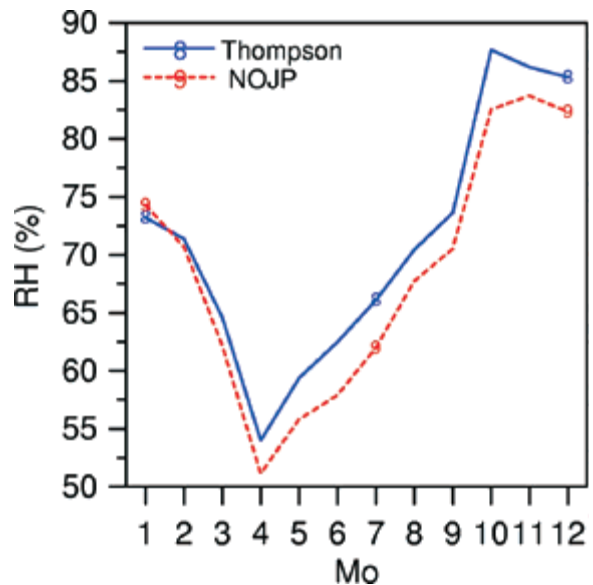


Fig. A.58. Annual cycle of relative humidity (1: January)

early winter, when the surface refreezes. Water is not available for transpiration in spring until the ground melts or for evaporation until the ground, wetlands and lakes warm with respect to the atmosphere. As discussed above, this leads to very low evaporative fraction in spring, with very large sensible heat fluxes from the forest canopy, which in turn produce deep dry boundary layers in spring. In autumn, when the lakes and ground are warm relative to the cooling atmosphere, the situation reverses. Evaporative fraction is high from the conifers and lakes, but low from deciduous species following senescence. Net radiation is much lower by the time the surface freezes, so sensible heat fluxes are very low and autumn boundary layers become very shallow, often capped by stratocumulus.

A.7.2.2 Effect of Land-cover Type on Seasonal Variation in Relative Humidity

At the BOREAS sites the dominant conifer species, black spruce, has a characteristic increase in evaporative fraction (EF), the ratio of latent heat to the sum of sensible and latent heat, from a minimum in spring to a maximum in late summer and autumn. Figure A.59 shows two sites for 1996 from the southern study area (Jarvis et al. 1997) and the northern study area (Goulden et al. 1997; Betts et al. 1999). Indeed this rise of evaporative fraction is responsible for the steady rise of mean relative humidity during the year as shown in Fig. A.58.

It can be thought of as a positive feedback between the surface ecological control and the relative humidity of the BL, since for black spruce, inferred vegetative resistance decreases almost linearly with increasing relative humidity (Betts et al. 1999). At deciduous and wetland sites there are both similarities and differences.

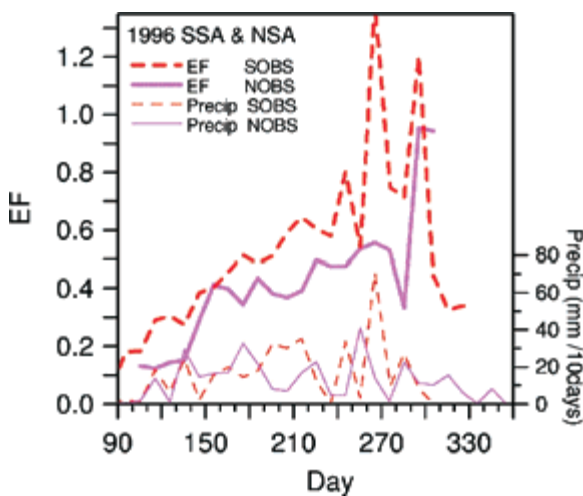


Fig. A.59. Black spruce evaporative fraction (EF) with corresponding 10-day precipitation

Figure A.60 shows the old aspen site in the southern study area (SOA: Blanken et al. 1997) and the fen site in the northern study area (NFen: Lafleur et al. 1997; Joiner et al. 1999b) for the same year. Once temperature climbs near the end of May (Day 150) (when the 10-day average temperature reaches 5 °C), latent heat flux rises rapidly at SOA, as leaf-out occurs. In mid-summer, evaporation is higher at the deciduous aspen site than at the spruce sites, but it is lower in the autumn than at the spruce sites, after the leaves die and fall. At the wetland site, NFen, the spring rise of evaporative fraction is also steep (there are some missing data), and there is a fall as the fen dries out in the summer. The leaf area index of the wetlands is lower and so transpiration (which can draw on a deeper root zone than surface evaporation) plays a less important role than at the aspen site.

A.7.2.3 Role of Stomatal Control

The well-known importance of the stomatal control of transpiration by a coniferous forest (e.g. Lindroth 1985; Jarvis and McNaughton 1986) was confirmed by BOREAS and NOPEX (Jarvis et al. 1997; McCaughey et al. 1997; Joiner et al. 1999a; Goulden et al. 1997; Betts et al. 1999; Cienciala et al. 1997, 1998, 1999; Grelle et al. 1999; Morén 1999). The diurnal cycle of evaporative fraction at the five flux sites in Fig. A.61 are quite different, even though there is little difference in the atmospheric forcing. At the Nfen, evaporative fraction climbs from mid-morning to mid-afternoon as evaporation increases with falling relative humidity. At the black spruce site, evaporative fraction does not rise as relative humidity falls to its afternoon minimum, indicating that stomatal control is playing a role. At this site evaporative fraction has a broad day-time minimum. At the jackpine site, where water is

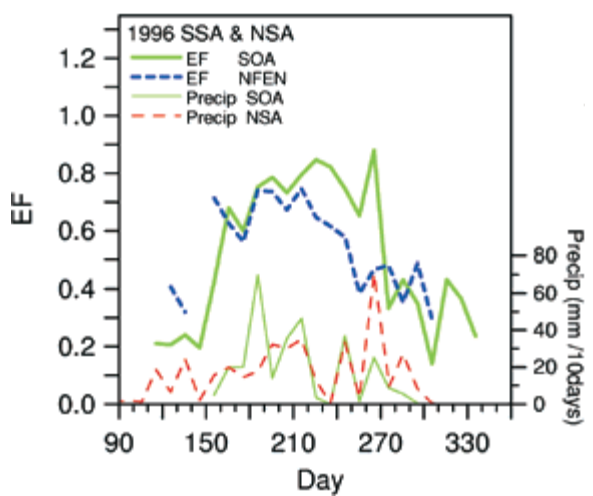


Fig. A.60. As Fig. A.59 for aspen and fen sites

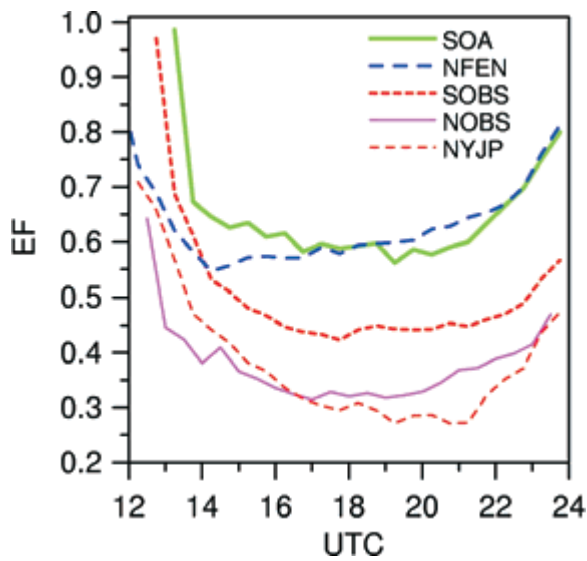


Fig. A.61. Summer day-time evaporative fraction (EF) for five flux sites (JJA 1996)

most limited because of the sandy soil, the solid curve shows that evaporative fraction drops to a minimum in mid-afternoon about the time of the relative humidity minimum. Here stomatal control must be the strongest. Figure A.62 (from Betts et al. 2001) illustrates this important climatic role even more clearly. We compare the link between measured evaporation from the NYJP and NFen sites, relative humidity and net radiation, by averaging the day-time data (1200–2400 UTC) from the months June to October of 1994 and 1996 into 10% bins in relative humidity, and 100 W m^{-2} bins of net radiation. During the day-time, the atmospheric forcing variables of temperature and humidity differ little between the sites, as discussed previously, but evaporation has a quite different behaviour. Evaporation increases with R_n as expected for both sites. At the fen, evaporation increases with decreasing relative humidity, consistent with the high availability of water. However, at the jackpine site, at low radiation levels, evaporation is flat with decreasing relative humidity, and at high radiation levels, evaporation actually falls as relative humidity decreases, showing that the sensitivity of stomatal control to relative humidity (or vapour pressure deficit) is the dominant process. So we see that at low relative humidity, the evaporation curves diverge widely, even though the atmospheric drivers are almost identical. Because the landscape is dominated by a forest with strong stomatal control, the climatic equilibrium of the diurnal cycle is controlled by the forest, not the fens. When evaporation is low, despite high R_n , relative humidity is low and the diurnal cycle of lifting condensation level (LCL) is large. The fens on the other hand are not in equilibrium with the overlying dry BL and have a much higher surface evapora-

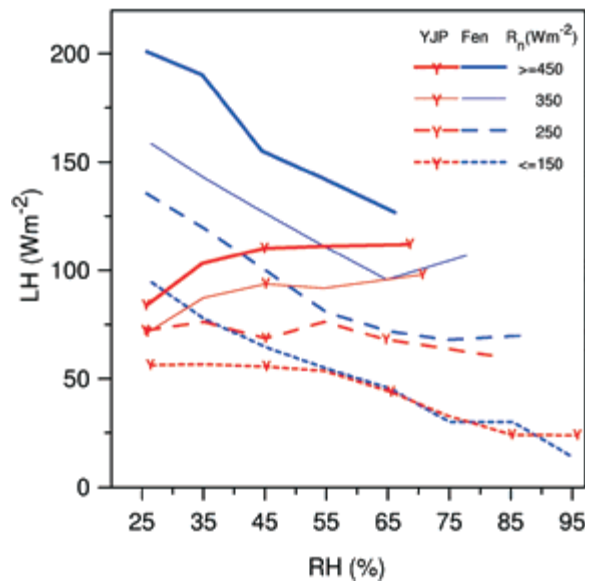


Fig. A.62. Distinct dependence of surface evaporation on relative humidity and net radiation at fen and jackpine sites

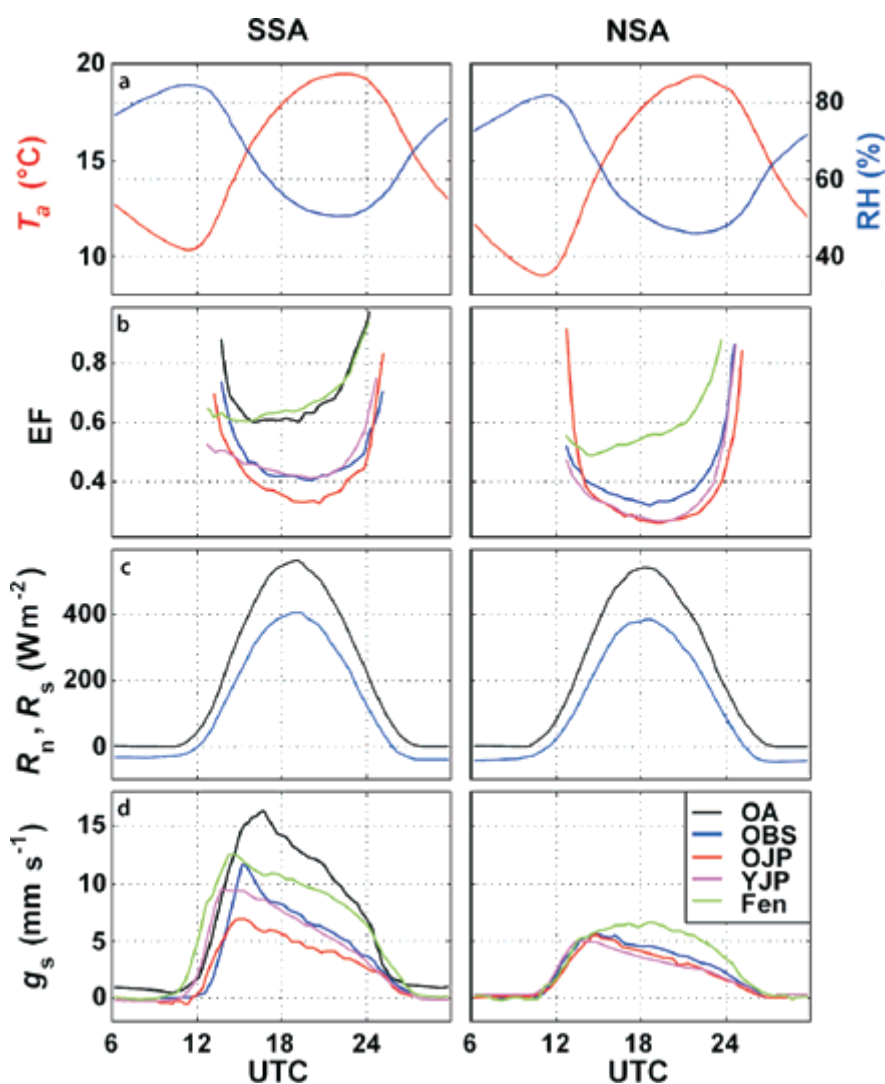
tion. We show the dependence of LH on relative humidity rather than vapour pressure deficit (VPD), which has been widely used in the study of canopy physiology, because VPD has a strong temperature dependence and the important atmospheric variables, relative humidity and LCL are tightly linked (Betts et al. 2001). In addition, Betts et al. (1999) found that vegetative resistance, inferred from data at the northern study area old black spruce site, was more tightly correlated with T and relative humidity than with T and VPD. The theoretical link between equilibrium evaporation, equilibrium BL depth and vegetative resistance is discussed more extensively in Betts (2000a). Other studies using branch bags (Rayment and Jarvis 1999) have shown that assimilation of CO_2 increases with light levels, decreases with increasing VPD, and has an optimum temperature range.

A.7.2.4 Role of Latitudinal Gradient

BOREAS had two study areas, at the north-east and south-west ends of a transect across the boreal forest. Figure A.63 from Barr et al. (2001) contrasts the BOREAS flux sites in the southern and northern study area. It compares the diurnal cycles (an average from 24 May to 19 Sept, 1994, corresponding essentially to the growing season) of (a) air temperature and relative humidity, (b) evaporative fraction, (c) solar and net radiation and (d) surface conductance. The meteorological variables are averaged over all sites. The *upper panels* show an afternoon maximum of temperature and a minimum of relative humidity. The *evaporative fraction panels* show a day-time minimum of evaporative fraction at all sites,

Fig. A.63.

Diurnal variation in air temperature, T_a (red lines), relative humidity: RH (blue lines), evaporative fraction, EF, solar radiation, R_s (black lines), net radiation, R_n (blue lines) and surface conductance to water vapour, g_s from BOREAS tower flux sites in the southern study area (SSA) and northern study area (NSA) averaged between 24 May and 19 Sept 1994. We first averaged the fluxes by time of day before calculating EF. The mean surface conductance was calculated from measured data only (e.g. with no gap filling) after excluding values below the 10th and above the 90th per-centiles. The line style is the same for each land-cover type. Local time in the southern and northern study area is 6 hours less than UTC (OA: old aspen; OBS: old black spruce; OJP: old jackpine; YJP: young jackpine)



with evaporative fraction at the southern study area exceeding evaporative fraction at the northern study area for each paired land cover. (Gaps in the data were filled using a model: see Barr et al. 2001.) In addition, the figure shows the characteristically different diurnal patterns of evaporative fraction for each land-cover type, independent of geographic location. At the fen sites, evaporative fraction increases as relative humidity falls from an early-morning maximum to a mid-afternoon minimum. At the aspen and old black spruce sites, the day-time pattern is relatively flat. At the jackpine sites, evaporative fraction falls the most and reaches the lowest afternoon minimum. These differences reflect the decreasing availability of water for evaporation and transpiration and the strongest stomatal control on transpiration at the jackpine sites. Mean relative humidity is a little lower for the northern than the southern study area, consistent with the uniformly lower evaporative fraction.

The southern-northern study area difference in evaporative fraction is consistent with the earlier results of

Barr and Betts (1997), who analysed the boundary-layer budgets of the BOREAS radiosondes. They reported mean mid-day Bowen ratios for the BOREAS northern and southern study area during the 1994 intensive field campaigns that correspond to evaporative fractions of 0.53 and 0.45, respectively. These values are intermediate between the lower conifer values and the higher aspen and fen values in Fig. A.63, and are about 30% higher than the mean mid-day values for mature black spruce (0.43 in the southern study area and 0.34 in the northern study area). These differences illustrate that, although the boreal forest landscape is dominated by conifers, particularly black spruce (Betts et al. 2001), its energy balance at the landscape scale is also influenced significantly by other land covers with higher evaporative fractions.

The lower panels in Fig. A.63 show the mean diurnal cycles of solar and net radiation (middle) and the derived surface conductance to water vapour (bottom). The southern study area aspen site has the highest surface conductance and the jackpine sites have the lowest. Un-

like the fen sites, where conductance is nearly symmetric with radiation (more so in the north than the south), the diurnal pattern of conductance is markedly asymmetric at the forest sites. The high forest conductances in the early-to-mid morning reflect the maximum daytime stomatal opening as a result of low-in-magnitude leaf water potentials, high relative humidity and low vapour pressure deficit (Margolis and Ryan 1997). At some sites and times, they may also reflect the presence of early-morning dew on the canopy. The fall of conductance between mid-morning and late afternoon at the forest sites reflects stomatal control as vapour pressure deficit increases (Margolis and Ryan 1997).

As was observed with EF, the paired sites (fen, old black spruce, old jackpine and young jackpine) each have higher mean conductance in the southern than in the northern study area. There is rather little difference in incoming short-wave radiation or in temperature between the northern and southern study area, and the 5% lower mid-day relative humidity in the northern study area is not sufficient to explain the significantly lower g_s . The higher rainfall in 1994 in the southern study area may explain part of the higher conductance, particularly at the jackpine sites. However, Betts et al. (2001) showed a similar difference between the black spruce sites in 1996, when rainfall was similar in both the southern and the northern study area. Thus, it is not likely that the seasonal atmospheric and soil water constraints between south and north are entirely responsible for the lower surface conductance in the north. Since g_s is a computed bulk stomatal conductance of the vegetated surface (rather than needle-level) the lower g_s in the north may be a result of lower canopy leaf area index.

A.7.2.5 Role of Moss

The wet conifer sites in BOREAS were characterised by extensive moss layers (Goulden et al. 1997; Price et al. 1997), which play an important role in the surface energetics and hydrology. The moss layer, typically tens of centimetres thick, is a thermal insulator, which limits the exchange of heat with the underlying mineral soil, and greatly reduces the annual range of soil temperature (see Fig. A.57 for site #8). In addition, the moss stores surface water after rainfall events, some of which drains and some of which is evaporated to the atmosphere. Price et al. (1997) estimated that about 23% of the precipitation throughfall was evaporated from the moss layer within a few days. Betts et al. (1999) found that evaporation for a black spruce site depended strongly on the wetness of the moss and canopy reservoirs. In contrast, variations in soil water in the underlying soil layer of the spruce root zone had no measurable effect on transpiration, probably because volumetric soil water never fell below 35% in this organic soil layer.

A.7.2.6 Role of Albedo of Forests, Wetlands and Lakes

The high latitude coniferous forests have a very low surface albedo in summer, around 0.08–0.09 for spruce and 0.09–0.13 for jackpine, and rather low values in winter, typically < 0.2 (Betts and Ball 1997), since the canopy shades the snow at low solar elevation angles. In contrast, more open wetland sites have much higher albedos in winter (Joiner et al. 1999b), as do the frozen lakes. The northern forests and wetlands are regions of sharply contrasting albedo, so this plays an important role on both short timescales and the annual timescale.

Figure A.64 shows daily average albedo from one year of the BOREAS mesonet data. In summer, the conifer sites have a very low albedo < 0.1 , comparable to the albedo of the lakes, while deciduous and grass sites have a significantly larger albedo. In winter the contrast is very large between forest (where the snow is beneath the canopy and shaded from the low sun angles, and albedo only rarely exceeds 0.2) and open sites and frozen lakes which can have albedos in the range 0.6–0.8, depending on the age of the snow. Errors in the mean albedo of the forest, wetland and lake system within Numerical Weather Prediction (NWP) models can have a large impact on surface temperature forecasts before snowmelt in spring (Viterbo and Betts 1999a). The length of the snow-free or unfrozen period has a marked impact on the annual net radiation balance of open areas and lakes at high latitudes, but less so for the forested areas, where the annual range of albedo is smaller. The presence of the low albedo forest may maintain a higher mean annual temperature than in a region at the same latitude without forest, even though snow melts earlier at open sites.

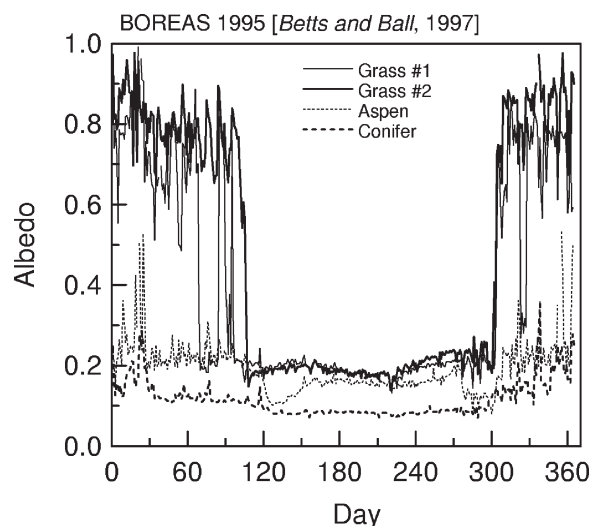


Fig. A.64. Daily average albedo, showing two grassland sites, an aspen site and an average of seven conifer sites (from Betts and Ball 1997, © American Geophysical Union)

Other studies have also indicated the importance of properly representing surface albedo in the snow-covered winter. For example, NWP simulations by Melas et al. (2001), incorporating a land-surface scheme based on Deardorff (1978), were used to study the diurnal variation of the boundary layer structure and surface fluxes during four consecutive days with air temperatures well below zero, snow-covered ground and changing synoptic forcing. Model results were evaluated against *in situ* measurements performed during the NOPEX winter field campaign in the northern NOPEX study area in Sodankylä, Northern Finland, in March 1997 (Gryning et al. 1999). The results show that the land-surface parameterisation employed in the NWP did not estimate day-time sensible heat fluxes correctly, in particular underestimating a pronounced afternoon maximum. This drawback was to a large extent removed by the implementation of a shading factor, as discussed in Gryning et al. (1999), to more accurately account for canopy heating resulting from increased interception of solar radiation at low solar elevations and the implementation of an objective heat storage scheme.

A.7.2.7 Role of Fire-induced Atmospheric Aerosols

Smoke aerosols produced by forest fires modify regional climate (Anderson et al. 1996; Charlson 1997) by (i) increasing cloud albedo, (ii) reducing surface insolation and (iii) influencing cloud formation and precipitation tendencies. The introduction of small particles such as those produced by the biomass burning in the boreal forest, common during the Canadian summer, have been shown to increase cloud albedo by acting as auxiliary cloud condensation nuclei, (Facchini et al. 1999). For the same water content, the average droplet size will diminish as the available number of activated cloud condensation nuclei increases, and the reflectivity of the cloud is consequently enhanced. This same effect also decreases the likelihood that the size threshold for precipitation will be encountered, potentially diminishing or suppressing precipitation in the affected regions (Rosenfeld 1998, 2000b). In addition, the heating of the troposphere as incident solar energy is absorbed by suspended smoke particles typically decreases the environmental lapse rate, and inhibits convective cloud development. This suppression of warm rain processes by heavy smoke conditions has been demonstrated conclusively by the Tropical Rainfall Measuring Mission (TRMM) observations (Rosenfeld 1999).

Fire-induced atmospheric aerosols also can reduce irradiance received at the surface. The single scatter albedo is a measure of the bulk absorption of an aerosol layer that ranges from 0.0–1.0 with lower values representing greater absorption by the aerosol. Observed single scatter albedo values derived from Cimel sunpho-

tometers at five sites in the Canadian boreal forest during 1994 and 1995 averaged 0.95 (standard deviation of 0.03). While these single scatter albedo values are somewhat higher than those typical for biomass burning, they still indicate a substantial reduction in received insolation due to aerosol absorption.

As the background (non-burning) aerosol loadings were typically of the order of 0.1 (aerosol optical thickness at 500 nm), the burning season produces a major modification of the radiation balance with bi-weekly average aerosol optical thicknesses as high as 1.0 for some intervals. This represents a reduction in received photosynthetically active radiation (PAR) irradiance at the surface of approximately 20% for mid-day conditions for a prolonged duration.

Gu et al. (2003) found that volcanic aerosols from the 1991 Mount Pinatubo eruption greatly increased diffuse radiation worldwide for the following 2 years and estimated that this increase in diffuse radiation alone enhanced noontime photosynthesis of a deciduous forest by 23% in 1992 and 8% in 1993 under cloudless conditions. They concluded that “the aerosol-induced increase in diffuse radiation by the volcano enhanced the terrestrial carbon sink and contributed to the temporary decline in the growth rate of atmospheric carbon dioxide after the eruption.”

A.7.2.8 Role of Surface Hydrology

Boreal hydrology plays a significant role in both surface energy balance and carbon cycling (see Sect. A.7.3). Evapotranspiration is limited by energy and water availability over much of the year (see Fig. A.56). This constraint tends to increase annual runoff ratios (ratio of annual runoff to annual precipitation). Even though the boreal forest would be a desert on the basis of annual precipitation alone, evaporative demand is low enough that runoff ratios are quite high. The excess of precipitation saturates large regions of clay soils with relatively little topography, creating the great boreal wetlands: lakes, bogs, fens, marshes and forested peatlands. These forested peatlands grow atop relatively shallow water tables (mostly < 40 cm) capped from beneath by an impermeable clay horizon, with black spruce and tamarack rooted in peat soils, kept moist throughout the growing season by a thick moss layer and low evapotranspiration rates ($\sim 2 \text{ mm d}^{-1}$). Nutrient cycling in this cool, moist root layer is slow, supporting only a sparse above-ground vegetation canopy (low leaf area index) with concomitantly low photosynthetic and evapotranspiration rates. Combined with limited energy availability, this results in a relatively low summertime evaporative fraction and relative humidity (see Fig. A.58–A.62), even during the growing season. Because of the low evapotranspiration rates over land, and the extensive area of lakes, open

water plays an important role in the energy balance of the region. Venäläinen et al. (1999), found that while latent heat fluxes from the forest exceeded that from lakes in late spring and early summer, in the boreal region of Sweden and Finland in late summer, lake values exceeded those of the forest. Furthermore, whereas night-time latent heat flux was essentially zero from the forest, it was significant from lakes throughout the summer. These features, along with relatively large areal coverage by lakes, wetlands and fens (especially in the North American boreal forest) also result in a highly damped stream flow from snowmelt runoff and occasional intense summer precipitation. Representation of these effects of surface storage on water and energy balances is a key feature of boreal hydrology that is not presently well represented in land-surface models.

Boreal hydrology also supports an important carbon storage generation mechanism in the spruce/tamarack wetlands, bogs and fens. Runoff storage in the wetland peats leads to low decomposition rates below ground with high root turnover, resulting in carbon storage rates ranging from 30 to 160 g C m⁻² y⁻¹ (e.g. Gorham 1991; Trumbore et al. 1999; Alm et al. 1997). Depending on the degree of soil saturation, anaerobic decomposition of organic materials in the boreal wetlands can generate methane (see Sect. A.7.3.5). Very wet sites, such as peatlands and beaver ponds, are generally sources of methane, ranging from 0–20 mg CH₄ m⁻² d⁻¹ for frozen palsas² and peat plateaus to ~380 mg CH₄ m⁻² d⁻¹ for open, graminoid fen sites (Bubier et al. 1995). Forested peatlands are generally associated with drier conditions and lower methane emission rates; permafrost collapse scars are associated with wet conditions and higher emission rates (Bubier et al. 1995). Beaver ponds emit both methane and carbon of about 50–150 mg CH₄ m⁻² d⁻¹, and carbon dioxide fluxes of about 2–10 g CH₄ m⁻² d⁻¹ (Roulet et al. 1997).

In wintertime, snow plays a central role in boreal hydrology. Even although the total fraction of annual precipitation that falls as snow in boreal forests is often well less than half, spring snow accumulations commonly account for much more than half of the annual runoff (see Bowling et al. 2000, for a map of this fraction over the Arctic drainage basin). Winter snowpacks, although present for much of the year, are usually quite thin, because temperatures are so low that relatively little precipitation occurs during the coldest mid-winter months. Because the snowpacks are quite thin, snow redistribution by wind, and accompanying sublimation, are important processes that affect peak snow accumulations at the onset of spring snowmelt. By some estimates (Pomeroy

et al. 1997) sublimation can result in a loss of one-third or more of the winter snow accumulation.

BOREAS results suggest that the fraction of runoff originating as snow is highest near the northern boundary of the boreal forest. At the gauged streams in the BOREAS northern study area, for instance, there was always a well-defined spring snowmelt peak in the seasonal hydrographs, whereas in the southern study area near the southern boreal forest boundary, the spring peak was less distinct, and in some years accounted for only a modest fraction of the annual runoff.

A.7.2.9 Scaling Energy and Water Flux from the Plot to the Region

The last few years of field measurements of energy, water and heat fluxes at scales of a kilometre or less, over relatively homogeneous surfaces, have resulted in the evaluation and refinement of soil-vegetation-atmosphere transfer schemes (SVATs) that permit reasonably accurate computation of energy, water and heat fluxes from the surface to the atmosphere. These models use as input, incident radiation, land cover structural characteristics and vegetation biophysics. SVAT models that represent these surface processes correctly are critical to the performance of boundary layer dynamics models that compute boundary layer properties as a function of surface conditions. These boundary layer properties are in turn crucial to parameterising general circulation models of the atmosphere, GCMs. Accurate GCMs are necessary to understand the relationships between climate and vegetation at global scales.

Even though the resolution of GCMs is steadily falling (the ECMWF 10-day forecast model has a current resolution of 40 km), GCMs must somehow either incorporate or ignore the effects of a heterogeneous landscape on surface fluxes. However, questions arise as to whether the average properties of a heterogeneous surface, used as input to a one-dimensional SVAT model, will compute energy, water and heat fluxes properly over the heterogeneous surface. A number of scaling studies have investigated this question. One strategy that has been employed is tiling (Koster and Suarez 1992; Van den Hurk et al. 2000).

Batchvarova et al. (2001) have shown that even a sparse canopy coverage by trees may have an influence on the area-averaged fluxes of momentum out of proportion to the area covered by the sparse trees, indicating that area averaging of surface roughness is a process that requires attention. The heat fluxes may be influenced to such a degree that the area-average heat flux may run counter to the area-averaged potential temperature gradient.

The regional sensible heat flux over the southern NOPEX experimental area, an inhomogeneous region with patches of forest, agricultural fields, mires and lakes

² Palsa is a type of wetland created when permafrost melts beneath the soil and creates a collapse of the land above the permafrost. These collapsed “scars” generally are circular, sunken beneath their surroundings, are poorly drained, thus support a unique type of vegetation such as brown moss.

at the southern boundary of the boreal zone, was estimated for three days of the campaign in 1994 (Gryning and Batchvarova 1999). It was found to be lower than the heat flux over forest and higher than the heat flux over agricultural fields. The regional sensible heat flux estimated by the mixed-layer evolution method was compared to a land use-weighted average sensible heat flux. The two independent estimates of the regional heat flux were found to be in general agreement. This result is supported by the findings of Gottschalk et al. (1999).

Based on measurements from the NOPEX winter experiment Batchvarova et al. (2001) estimated the regional (aggregated) momentum and sensible heat fluxes for two days over a site in Finnish Lapland during the late part of the winter. The study shows that the forest dominates and controls the regional fluxes of momentum and sensible heat in different ways. The regional momentum flux was found to be only slightly smaller than the measured momentum flux over the forest, although the forest (deciduous and coniferous) covered only 49% of the area. The regional sensible heat flux was estimated to be 30 to 50% of the values measured over a coniferous forest. This percentage corresponds roughly to the areal coverage of coniferous forest in the area (see Chapt. B.10 for further discussion).

A.7.3 Biospheric Carbon Exchange: Carbon Dioxide and Methane

The major terms in the net carbon balance of a boreal ecosystem are carbon uptake via photosynthesis (gross primary productivity, GPP), carbon loss by the autotrophic respiration of vegetation (R_a), and carbon loss by heterotrophic respiration (R_h) of decomposers. The net carbon assimilation by the vegetation is called net primary production ($NPP = GPP - R_a$). In boreal forest ecosystems R_a is typically more than 50% of GPP (Ryan et al. 1997). Net ecosystem exchange (NEE) is equal to net uptake by vegetation minus release by decomposition:

$$NEE = NPP - R_h = GPP - R_a - R_h \quad (\text{A.14})$$

NEE is generally a small difference between much larger gross photosynthesis and respiration, and can be near zero for some mature forest stands (e.g. Goulden et al. 1997). Additional pathways of carbon loss from boreal ecosystems are generally either small or very large but episodic. The smaller pathways include volatile organic carbon (VOC) emissions from foliage (Lerdau et al. 1997) and dissolved organic and inorganic carbon (DOC and DIC) losses with groundwater flow (e.g. Aitkenhead and McDowell 2000). The larger but episodic pathways include harvest and fire.

A.7.3.1 Measurement Methods

Ecosystem carbon balances can be measured in three fundamentally independent ways (Table A.8): (i) eddy correlation methods, (ii) carbon stock methods or (iii) the inverse method.

The eddy correlation method places high frequency sonic anemometers and gas sampling inlets above the canopy, and correlates variance in CO_2 concentrations with variance in vertical air motion to assess net CO_2 flux between the canopy and the atmosphere (e.g. Wofsy et al. 1993). In theory, near-continuous measurements of CO_2 exchange can be integrated to determine NEE over a measurement period. In practice, there are a number of challenges and uncertainties associated with the eddy correlation method (e.g. Goulden et al. 1996; Grelle and Lindroth 1994, 1996). The eddy correlation method provides a very good picture of how the ecosystem responds to weather at hourly to seasonal time scales, and is an important tool for developing and evaluating process-based ecosystem models. See Chapt. B.4 for further description of this methodology.

The carbon stock method requires actual measurement of the carbon in soils and vegetation at a number of stands. In principle, net carbon sequestration at a site can be measured directly if a site is visited repeatedly over a number of years. However, net sequestration is often a very small fraction of the standing carbon stocks, and thus sequestration can be difficult to detect. Often,

Table A.8. Methods for assessing ecosystem carbon balance

	Eddy correlation method	Carbon stock method	Inverse method
Observation	Net carbon fluxes	Carbon in biomass and soils	Atmospheric [CO_2], transport, sources
Inference	Net C sequestration	Net C flux	Net C flux and sequestration
Measurement effort	Intensive	Extensive	Very extensive
Characterise ecophysiology	Yes	No	No
Disaggregate components	Possible with enough measurements	Yes	No
Other uses	Process model validation and parameterisation	Chronosequences: ecosystem evolution	Regional view, large scale evaluation

stand-age chronosequences are measured and carbon sequestration is inferred from these data under the assumption that all sites have followed or will follow a similar successional/developmental trajectory (e.g. Rapalee et al. 1998). This carbon stock method can provide information on the contributions of the different components of the ecosystem (trees, mosses and ground vegetation, soils) to total carbon pools and carbon sequestration.

The inverse method combines observed gradients in atmospheric CO₂ concentration and isotopic ratios, modelled or measured atmospheric transport, and known anthropogenic CO₂ sources to infer net CO₂ exchange at the land surface (e.g. Heimann and Kaminsky 1999). As the current network of atmospheric data is very large-scale (e.g. continental or larger), only inferences can be made (e.g. Fan et al. 1998). However, both the other methods are quite localised, so the inverse method provides a meaningful constraint on regional carbon fluxes. Ultimately, the three methods should be consistent with, and constrain, each other.

A.7.3.2 Controlling Factors (above and below Ground)

Rates of photosynthesis, respiration, and decomposition have a number of biophysical and ecological controls. Controls on seasonal and interannual variability are discussed in Sect. A.7.3.4. Base photosynthetic rates for foliar tissue are generally correlated with foliar nitrogen content (e.g. Field and Mooney 1986; Reich et al. 1997; Dang et al. 1997). Needle-leaf evergreen trees, which dominate the boreal forest, generally have low tissue nitrogen content and low photosynthetic rates (e.g. Reich et al. 1997). *GPP* and *NEE* rates for boreal peatlands are generally lower than for temperate ecosystems (Frolking et al. 1998). Incident PAR has a very strong control on photosynthetic rates, both over a diurnal cycle, and on day-to-day variability (e.g. Goulden et al. 1997; Suyker et al. 1997; Jarvis et al. 1997; Joiner et al. 1999a). Vapour pressure deficits greater than about 1 kPa have been shown to cause stomatal closure and limit photosynthetic and transpiration rates for boreal trees (Dang et al. 1997; Hogg and Hurdle 1997; Hogg et al. 1997; see also Sect. A.7.2.3). However, a strong vapour pressure deficit control on *NEE* and *GPP* of black spruce (*Picea mariana* (Mill.) BSP) stands was not observed (e.g. Jarvis et al. 1997; Goulden et al. 1997).

Lavigne et al. (1997) estimated that, for six coniferous boreal stands, soil respiration (roots plus heterotrophs) was ~ 50–70% of total ecosystem respiration; foliar respiration was ~ 25–40% of total ecosystem respiration, and above-ground woody tissue respiration was ~ 5–15% of total ecosystem respiration. Ryan et al. (1997) estimated

that root respiration was about half of total autotrophic respiration. All respiration rates showed temperature dependence with Q₁₀ values (i.e. rate increases for a 10 °C temperature increase) of ~ 1.5 for wood, ~ 1.9 for roots, and ~ 2.0 for foliage (Ryan et al. 1997). Goulden et al. (1997) fit an exponential function to total ecosystem respiration as measured by eddy correlation in a boreal black spruce stand that is equivalent to a Q₁₀ value of about 2.0. Savage et al. (1997) reported a Q₁₀ value of 2.6 for temperature dependence of soil respiration measured with manual chambers in the same black spruce stand. Goulden and Crill (1997) reported a Q₁₀ value of about 2.0, based on automated chamber measurements in this stand. Bubier et al. (1998) reported Q₁₀ values of 3.0 to 4.1 for a range of peatland sites using chamber measurements. Water table is also an important control on respiration in boreal wetlands because of slower rates of CO₂ emission in anaerobic conditions (Moore and Dalva 1993; Silvola et al. 1996; Bubier et al. 1998). Peatlands can switch from being a net sink of carbon to being a net source in exceptionally dry periods due to increased aerobic respiration rates (Alm et al. 1999; Bellisario et al. 1998).

A.7.3.3 Geographic Variations in Carbon Flux

Above-ground NPP (ANPP) rates of 120–350 g C m⁻² y⁻¹ were measured for forest stands in the BOREAS study area in central Canada, within the range of data from a number of boreal sites around the world (Gower et al. 1997). There are fewer estimates of below-ground NPP for boreal forests, but Steele et al. (1997) and Ruess et al. (1996) estimated fine root NPP to be roughly 50–100% of above-ground litterfall for deciduous stands and 100–200% of above-ground litterfall for evergreen stands in North America. Analysing eddy correlation carbon flux data from a network of towers ranging from northern to southern Europe, Valentini et al. (2000) concluded that much of the observed variation in *NEE* between these sites was due to differences in net ecosystem respiration, while *GPP* was fairly uniform across the sites. Ecosystem respiration generally increased, south to north, from roughly 50% to nearly 100% of *GPP*. Valentini et al. (2000) postulated that this may be due to enhanced Rh as a result of a disequilibrium in soil organic matter pools at the more northern sites, due both to climatic warming and site disturbances. At an evergreen boreal stand in Canada, Goulden et al. (1998) observed high ecosystem respiration during a warm summer, which they attributed primarily to anomalous warming/thawing of soil organic matter about 0.5–1.0 m below the surface. However, at a deciduous boreal stand in Canada, Black et al. (2000) observed very little variation in the annual total ecosystem respiration over four years, despite ~ 3.5 °C variation in mean annual temperature.

Lindroth et al. (1998) and Morén (1999) measured CO₂ fluxes using eddy correlation above a mixed pine and spruce forest in central Sweden during a two-year period, from June 1994 to May 1996. During that period, the forest was observed to be a net source of carbon. Analysis of night-time fluxes showed that 79% of the variation in night-time CO₂ respiration could be explained by an exponential temperature function. Using this function to estimate respiration during day-time allowed gross uptake to be estimated as well. In 1995, the gross uptake was $\sim 1250 \text{ g C m}^{-2} \text{ y}^{-1}$ and the total ecosystem respiration was $\sim 1500 \text{ g C m}^{-2} \text{ y}^{-1}$. Typical eddy correlation measurements of growing season, mid-day NEE for boreal ecosystems are an uptake of $3\text{--}25 \text{ g CO}_2 \text{ m}^{-2} \text{ y}^{-1}$ (e.g. Sellers et al. 1997; Lindroth et al. 1998).

Millennial-scale carbon sequestration rates in peatlands have been estimated by dividing total carbon content by basal age, and average about $30 \text{ g C m}^{-2} \text{ y}^{-1}$ (e.g. Gorham 1991). Using three different methods Trumbore et al. (1999) estimated C sequestration rates of $0\text{--}160 \text{ g C m}^{-2} \text{ y}^{-1}$ for different components of a boreal peatland in central Manitoba, Canada. Alm et al. (1997) used the static chamber method to measure a mean C sequestration rate of about $70 \text{ g C m}^{-2} \text{ y}^{-1}$ for a boreal peatland in Finland. Estimates of boreal peatland ANPP range from about 100 to $500 \text{ g C m}^{-2} \text{ y}^{-1}$ (e.g. Trumbore et al. 1999; Thormann and Bayley 1997). There are few measurements of below-ground NPP for peatlands (e.g. Backéus 1990; Saarinen 1996), and estimates must be considered extremely uncertain.

Regional-scale rates of NEE, NPP, and methane flux are very difficult to measure, due to the large spatial and temporal domains needed. Typical eddy correlation towers generate a long time series but sample only a relative small area ($< 1 \text{ km}^2$) (see Sect. B.4.3.4). Eddy correlation instrumentation on aircraft can cover larger spatial domains but generally have very poor temporal coverage (see Chapt. B.5). Atmospheric sampling of CO₂ concentrations, combined with inverse modelling, can represent large area and time domains but with poor temporal and spatial resolution. Combining land-cover maps derived from remote sensing (e.g. Steyaert et al. 1997) with ecosystem models has been used to generate regional flux estimates of CO₂ (e.g. Liu et al. 1999b). Similarly, combining remote sensing land-cover maps with site level flux data has been used to generate regional methane flux estimates (Roulet et al. 1994; Reeburgh et al. 1998). In a model scaling exercise, Kimball et al. (1999) showed that results were sensitive to the scale of resolution of the landscape complexity. Small landscape features that can have large fluxes (e.g. beaver ponds for CO₂ and CH₄, peatlands for CH₄) can be difficult to resolve and quantify at the landscape scale, and can thus lead to significant uncertainty in regional analyses. Rates and intensity of disturbance of boreal ecosystems by fire,

insect defoliation, harvest, or permafrost degradation will also have a significant impact on the regional carbon balance in any year, and on the long-term carbon balance of any site (e.g. Harden et al. (1997); also see papers in Apps and Price (1996), and Apps et al. (1995)). These effects are not well quantified at this time.

A.7.3.4 Seasonal and Interannual Variations in Carbon Flux

Ecosystem carbon fluxes show a strong seasonal signal, with maximum uptake rates in early and mid-summer, and maximum loss rates in early autumn and late spring. Boreal field sites with year-round eddy correlation observations show low but persistent and significant net loss of carbon throughout the long, cold winter months (Goulden et al. 1997; Lindroth et al. 1998; Black et al. 2000). Winter soil flux measurements show that much of this respiration comes from below-ground and is highly variable, both spatially and temporally (Winston et al. 1997). Dormant season Ra accounts for about one-quarter of yearly total plant respiration (Ryan et al. 1997).

Eddy correlation measurements of CO₂ exchange have been made at a number of boreal stands, but only a few sites have reported near-continuous, year-round data for more than one year. After two years of eddy correlation measurements at a mature pine and spruce forest in central Sweden, Lindroth et al. (1998) estimated a net loss of about $200 \text{ g C m}^{-2} \text{ y}^{-1}$. They postulated that the forest cannot sustain a persistent loss of C at these rates, and that the two years of observation may have been anomalous due to a dry summer in one year reducing photosynthesis, and to some anomalously warm months enhancing respiration. After nearly two and a half years of eddy correlation measurements at a mature spruce stand in central Manitoba, Canada, Goulden et al. (1997) estimated that the gross photosynthesis and total respiration were nearly in balance at about $800 \text{ g C m}^{-2} \text{ y}^{-1}$ each. Despite being an evergreen forest, gross photosynthesis was quite low and insensitive to air temperatures ranging from -10 to $+10$ °C during April, before the ground had thawed. Gross photosynthesis increased with increasing air temperature during May–October. After four complete years of eddy correlation measurements at a boreal deciduous forest in central Saskatchewan, Canada, Black et al. (2000) reported net carbon sequestration of 80 to $290 \text{ g C m}^{-2} \text{ y}^{-1}$. A warm, early spring in 1998 caused an earlier leaf-out, and these additional two to four weeks of active photosynthesis led to the large NEE, more than double that of the other three years. Total ecosystem respiration in 1998 was similar to the other three years (Black et al. 2000). Measurements at the black spruce forest in Manitoba also showed an early start to the active growing season in 1998, and

annual NEE at the site switched from a weak carbon source to a weak carbon sink for that year (Steve Wofsy, pers. comn.). Because the annual air temperature wave lags the annual insolation wave by about a month at these latitudes, by the time boreal ecosystems thaw in spring, light levels are quite high. In addition, the ecosystems warm rapidly and water is abundant, so net productivity can be high early in the active growing season. By contrast, when ecosystems freeze-up in the autumn (October–November) light levels and photosynthesis rates are low. Thus gross productivity is much more sensitive to variation in the timing of spring thaw than autumn freeze-up (Frolking 1997).

A.7.3.5 Methane

Four primary controls on methane fluxes have been identified. Net methane emission generally increases with increasing soil temperature, with increasing soil moisture and/or shallower water tables, with increasing conductance through plant aerenchymous tissue, and with increasing substrate availability (e.g. Crill et al. 1991; Chanton and Dacey 1991). For upland soils that are net consumers of atmospheric methane, the primary control of fluxes rates is gas diffusion rates, which are closely related to soil moisture content. For peatlands that are net emitters of methane, Bubier et al. (1995) found that mean seasonal peat temperature at the average position of the water table explained most of the spatial variability in mean seasonal CH_4 fluxes for a diverse peatland

complex in Manitoba, Canada. Vegetation assemblages are generally correlated with the biophysical controlling factors, and can be useful for scaling flux estimates to larger regions (Bubier et al. 1995). Net ecosystem production is a good predictor of methane emission in flooded wetland soils (Whiting and Chanton 1993), but this relationship weakens when the water table is below the surface of the peat (Bellisario et al. 1998).

Methane is both produced and consumed by microbial processes in boreal soils. Boreal ecosystem methane uptake rates measured with static chambers in drier upland soils ($\sim 0.1\text{--}1.0 \text{ mg CH}_4 \text{ m}^{-2} \text{ d}^{-1}$; e.g. Moosavi and Crill 1997; Savage et al. 1997) are generally comparable to rates in other ecosystems. Continuous methane flux measurements over a five-month growing season at an aspen stand in Saskatchewan, Canada, using a micrometeorological tower and the flux-gradient method, averaged an uptake of about $1.4 \text{ mg CH}_4 \text{ m}^{-2} \text{ d}^{-1}$ (Simpson et al. 1997). Wetter sites can exhibit episodes of methane emission and methane uptake, generally depending on degree of soil saturation (e.g. Moosavi and Crill 1997; Simpson et al. 1997). Very wet sites, such as peatlands and beaver ponds, generally are net sources of methane (e.g. Bubier et al. 1995; Roulet et al. 1997; Moore and Roulet 1993). Seasonal average emission rates from a peatland complex in Manitoba, Canada ranged from $0\text{--}20 \text{ mg CH}_4 \text{ m}^{-2} \text{ d}^{-1}$ for frozen palsas and peat plateaux to $\sim 380 \text{ mg CH}_4 \text{ m}^{-2} \text{ d}^{-1}$ for open, graminoid fen sites (Bubier et al. 1995). Forested peatlands are generally associated with drier conditions and lower methane emission rates; permafrost collapse scars are associated with wet conditions and higher emission rates (Bubier et al. 1995). Beaver ponds emit both methane and carbon dioxide; Roulet et al. (1997) using a micrometeorological tower and the flux-gradient method, measured methane emission rates of about $50\text{--}150 \text{ mg CH}_4 \text{ m}^{-2} \text{ d}^{-1}$, and carbon dioxide fluxes of about $2\text{--}10 \text{ g CO}_2 \text{ m}^{-2} \text{ d}^{-1}$.

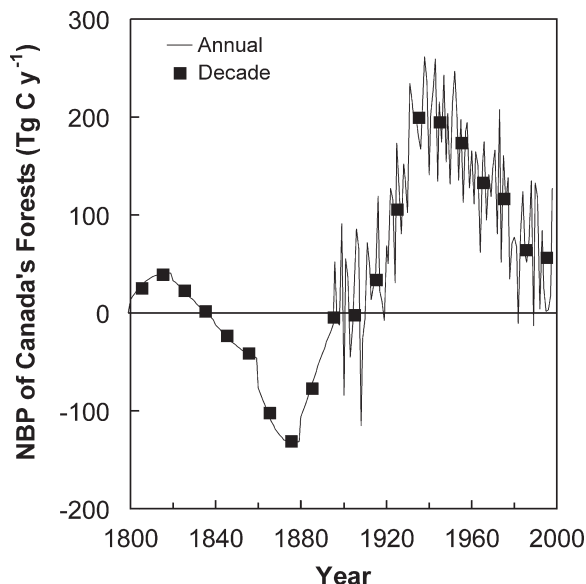


Fig. A.65. Net biome productivity (NBP) in Canada's forests for the last two centuries (expanded after Chen et al. 2000). In the estimate, disturbance (fire, insect-induced mortality, harvest) and non-disturbance (temperature, growing season length, nitrogen deposition, CO_2 fertilisation) factors are considered

A.7.3.6 The Effect of Landscape Patterns, Disturbance and Succession on Carbon Cycling

As shown in Fig. A.65, the high disturbance rates in late 19th century caused Canada's forests to release C at a rate of $\sim 30\text{--}120 \text{ Tg C y}^{-1}$ (Chen et al. 2000). During 1930–1970 the low disturbance rates, in combination with forest regrowth in areas disturbed in the late 19th century, allowed Canada's forests to uptake C at a rate of $\sim 100\text{--}200 \text{ Tg C y}^{-1}$. The increased disturbances during 1980–1996 released 60 Tg C y^{-1} from Canada's forests. Similar results were reported by Kurz et al. (1995). However, the positive effects on forest growth of nitrogen deposition, enhanced nitrogen mineralisation and increased growing season length with increasing temperature and increased atmospheric CO_2 concentration might have outweighed the negative effects of the increase in

disturbance rates in recent decades, making Canada's forests currently a small sink of $\sim 50 \text{ Tg C y}^{-1}$ on average (Chen et al. 2000). Among the four disturbance factors, fire had the most important contribution to the inter-annual and decadal variations of net biome productivity (NBP), followed by insect-induced mortality.

A.7.4 Sensitivity Experiments

Climate model sensitivity simulations of the response to increasing atmospheric CO_2 concentrations indicate that the rapid warming could occur at these high latitudes ($43\text{--}65^\circ \text{N}$) with the most marked effects within the continental interiors, see Houghton et al. (1995), Mitchell (1983), Schlesinger and Mitchell (1987), Sellers et al. (1996a). Analyses of long-term, ground-measured surface temperature records are consistent with these model simulations, showing increasing temperature trends of as much as 1.25°C per decade (Chapman and Walsh 1993) with much of this warming occurring in the spring and fall.

Such perturbations in northern continental climates could well lead to significant changes in the carbon cycle and the ecological functioning of the boreal forest, which could feedback onto the global climate. The boreal ecosystem may be responding to such warming by increasing vegetation growth. Studies by Keeling et al. (1996) have found recent increases in the amplitude of the atmospheric CO_2 concentration and a broadening of the seasonal cycle by as much as six days, suggesting increased vegetation growth. Results from BOREAS indicate that an earlier onset of spring photosynthetic activity leads to large increases in annual vegetative carbon uptake (Sellers et al. 1997). Satellite studies of high latitude vegetation show concomitant increases in both leaf area duration and vegetation density (Myneni et al. 1997) over the past decade.

However, an increasingly warm, dry boreal climate could potentially shift the ecosystem from being a net sink of carbon to a net source. Results from BOREAS (Hall 1999) and NOPEX (Halldin et al. 1999) also show that if climate warming leads to drying and warming of the boreal soils, accelerated decomposition of the organic matter stored in the peat soils and organic soil horizons could potentially release huge quantities of stored soil carbon to the atmosphere (Sellers et al. 1997; Lindroth et al. 1998).

A.7.4.1 Snow Albedo and Climate Feedback

A number of studies also indicate the influence of boreal land-surface/atmosphere interactions on global weather patterns and interannual variations in climate. For example, Viterbo and Betts (1999a) using the European

Centre for Medium-Range Weather Forecasts (ECMWF) model, showed that varying assumptions about the albedo of the snow-covered boreal ecosystem can lead to wide differences in spring temperature forecasts across North America and, in fact, throughout the Northern Hemisphere, Asia and the western Pacific.

The spring snow cover feedback mechanism observed by Groisman et al. (1994) in which decreased snow cover reduces surface albedo, increases surface absorption of radiation, raises surface temperatures, and hence increases snow melt, affects seasonal atmospheric circulation as well as long-term climate. As air temperatures warm, the snow cover feedback acts to either amplify the rate of retreat of the snow extent, and its seasonal duration, or mitigate it.

A.7.4.2 Carbon Sequestration and Radiative Feedbacks

Bounoua et al. (1999) used a coupled biosphere-atmosphere model to examine the radiative and physiological effects on climate from a doubling of the atmospheric carbon dioxide concentration. Their study demonstrated the importance of accounting for vegetation response to climate change. When only the radiative effects from doubled CO_2 were taken into account, a mean temperature increase of 2.6 K over land was predicted with a 7% increase in precipitation. However, the changes varied with latitude, with an increase of 4 K at boreal latitudes ($> 50^\circ \text{N}$), but only 1.7 K over the tropics. As the physiological effects of vegetation were added, the predicted temperature increase over land increased only slightly, but a smaller difference of 0.7 K was observed between the boreal and tropical latitudes. This smaller difference decreased evaporation and transpiration rates of land vegetation, a result of increased atmospheric CO_2 concentrations.

Other climate change sensitivity experiments also indicate that boreal latitudes could undergo warming, resulting in the extension of the frost-free season by one to nine weeks in North America (Brklacich et al. 1997). For the Prairies, Ontario and Québec, the model results suggest an extension of three to five weeks, while for Atlantic Canada near the current agricultural margin the season is three to four weeks longer. Air temperature during the frost-free season is also simulated to increase. Estimates related to agricultural moisture regimes show a broad range compared to the thermal regimes. For instance, in the Prairies and Peace River regions, simulated precipitation changes range from decreases of about 30% to increases of about 80%. As the frost-free season becomes longer and warmer, most model simulations suggest higher potential evaporation and transpiration rates and thus the larger seasonal soil moisture deficits (Brklacich et al. 1997).

A.7.4.3 Effects of Climate Change on Land Cover

Based on pollen records, species would shift northward with increasing temperatures (Oechel and Vourlitis 1994). In the northern regions, species richness would be reduced through the loss of less abundant species and a move to species characteristic of other biomes (Chapin et al. 1995). The area of boreal forest in Québec could decrease by as much as 20% (Singh 1988). Solomon and West (1987) simulated tree dynamics in north-western Ontario and found that the dominance of spruce slowly gave way to an increasing proportion of sugar maple and white pine that entered the canopy in a $2 \times \text{CO}_2$ sensitivity experiment. Plöchl and Cramer (1995) used an ecosystem model to locate tundra and taiga distributions under a $2 \times \text{CO}_2$ sensitivity experiment and suggested that both biomes will diminish in extent when forced to shift northward. Many of these simulations are based on equilibrium states, which may never be realised. More realistic estimates for land-cover changes (e.g. since industrialisation) in response to the past climate are not yet found in the literature.

In assessing the potential for agricultural expansion to areas in north-west Canada (i.e. north of 55°N and west of 110°W) and Alaska, Mills (1994) identified 57 Mha of potentially arable land. This estimate drops to 39 Mha when climatic limitations are imposed, but under a sensitivity experiment of $2 \times \text{CO}_2$ it increases to 55 Mha. Similar conclusions have been reached for the northern agricultural regions in Québec and Ontario (Brklacich et al. 1997). Agricultural land potential north of 60°N is generally considered not to be sensitive to these simulated climate changes.

The studies suggest that warmer frost-free seasons under the full range of global climatic change sensitivity experiments would increase the rate of development of grain crops, reducing the time between seeding and harvesting (e.g. by about one-and-one-half to three weeks in most regions of Canada for spring-seeded cereals and coarse grains) (Brklacich et al. 1997). In northern regions, the simulated decrease in maturation time would reduce the risk of frost-induced crop injury, a decided benefit for these regions. In the Peace River region, the positive and negative influences tend to counteract each other, reducing the magnitude of the positive impacts of climatic change on cereal yields. In the Prairies, the effects of climatic change on grain yields are more pronounced and variable, with spring-seeded cereal yields in the western Prairies reducing by as much as 35% and those in the eastern Prairies increasing by as much as 66%. Similar results are suggested for Ontario and Québec, except for the more generally positive impacts on grain production, especially corn, in northern Ontario and Québec.

A.7.4.4 Hydrological Feedbacks

The hydrology of boreal regions is particularly susceptible to climate (Bowling et al. 2000; Nijssen et al. 2001). Near the southern border of the boreal forest, winter snow accumulations, and hence spring runoff, might well decrease. However, parts of the boreal forest that now have extremely cold winters could see increased winter precipitation according to some climate models. This, in conjunction with earlier onset of spring, would change the seasonal flow of the northern rivers, most likely shifting peak runoff associated with spring snowmelt to earlier in the year, and possibly reducing summer flows. Furthermore, both short-term feedbacks in the climate – due to changes in albedo associated with variations in the length of snow cover, especially near the northern limit of the boreal forest, and tundra areas where vegetation effects on albedo are least – may well occur due to changes in the surface radiative balance, especially in spring. Likewise, changes in the amount of discharge, and the seasonality of runoff of the major north-flowing rivers, could affect the global thermohaline circulation, due to both direct effects on the freshwater balance and to indirect effects on albedo of ice-free portions of the Arctic Ocean. More local effects would almost certainly occur due to changes in depth of the active (seasonally thawed) layer in permafrost areas, which are particularly important near the northern boundary of the boreal forest. These fundamental changes in growing season length, and soil properties, would almost certainly affect the northern and southern boundaries of the boreal forest, which would have accompanying changes on surface hydrology.

During the summertime, increases in precipitation at northern latitudes (Dai et al. 1997) could also have significant impacts on boreal hydrology and, through the mechanisms discussed in Sect. A.7.2.8, surface energy balance and carbon cycling and storage rates. For example, if increased precipitation trends lead in the long-term to a shallower water table overall, nutrient cycling rates could potentially decrease further, leading to decreased summertime evapotranspiration. On the other hand, drying and warming of the boreal climate could lead to increases in the water table depth, increased above-ground productivity, but also increased decomposition rates of the peat soils. The balance between these two processes could potentially change the boreal ecosystem from a net sink to a net source of carbon, or vice versa. This potential coupling between subsurface hydrology, carbon, energy and water cycling needs to be explored further.

REFERENCES

- Aitkenhead JA, McDowell WH. 2000. Soil C:N ratio as a predictor of annual riverine DOC flux at local and global scales. *Global Biogeochem. Cycles*. 14:127-138.
- Alm J, Talanov A, Saarnio S, Silvola J, Ikkonen E, Aaltonen H, Nykänen H, Martikainen PJ. 1997. Reconstruction of the carbon balance for microsites in a boreal oligotrophic pine fen, Finland. *Oecologia*. 110:423-431.
- Alm, J. et al., 1999. Schulman L, Walden J, Nykänen H, Martikainen PJ and Silvola J. (manuscript) Carbon balance of a boreal bog during a year with an exceptionally dry summer. *Ecology* 80:161-174
- Apps M.J., Price DT (eds.), 1996. *Forest Ecosystems, Forest Management and the Global Carbon Cycle*. NATO ASI Series Vol .I-40. Springer, Berlin. 452 pp.
- Apps MJ, Price DT, Wisniewski J. (eds.) 1995. *Boreal Forests and Global Change*. Kluwer Academic. Dordrecht. 540 pp.
- Backéus I. 1990. Production and depth distribution of fine roots in a boreal open bog. *Ann. Bot. Fennici* 27:261-265.
- Barr, A. G., A. K. Betts , T.A. Black , J.H. McCaughey and C.S. Smith, 2000. Intercomparison of BOREAS Northern and Southern Study Area Surface Fluxes in 1994. Submitted to JGR BOREAS Special Issue
- Barr, A.G. and A.K. Betts, 1997. Radiosonde boundary-layer budgets above a boreal forest, *J. Geophys. Res.* 102:29,205-29,212.
- Batchvarova E., Gryning S. E. and Hasager C. B., 2000. Regional Fluxes of Momentum and Sensible Heat over a Sub-Arctic Landscape during Late Winter, *Boundary-Layer Meteorology*. Submitted.
- Batchvarova E., Sven-Erik Gryning and Charlotte Bay Hasager, submitted. Regional Fluxes of Momentum and Sensible Heat over a Sub-Arctic Landscape during Late Winter, *Boundary-Layer Meteorology*.
- Beaubien, J., J. Cihlar, G. Simard, and R. Latifovic. 1999. Land cover from multiple Thematic Mapper scenes using a new enhancement-classification methodology. *Journal of Geophysical Research* 104(D22): 27909-27920.
- Betts, A. K., J.H. Ball, Beljaars, A.C.M., M.J. Miller and P. Viterbo, 1996. The land-surface-atmosphere interaction: a review based on observational and global modelling perspectives. *J. Geophys. Res.* 101, 7209-7225.
- Betts, A. K., M. L. Goulden, and S.C. Wofsy, 1999a. Controls on evaporation in a boreal spruce forest. *J. Climate*, 12, 1601-1618.
- Black TA, Chen WJ, Barr AG, Arain MA, Chen Z, Nesic Z, Hogg EH, Neumann HH, Yang PC. 2000. Increased carbon sequestration by a boreal deciduous forest in years with a warm spring. *Geophys. Res. Lett.* 27:1271-1274.
- Blanken, P.D., T.A. Black, P.C. Yang, H.H. Neumann, Z. Nesic, R. Staebler, G. den Hartog, M.D. Novak, and X. Lee: 1997. Energy balance and canopy conductance of a boreal aspen forest: Partitioning overstory and understory components. *J. Geophys. Res.*, 10
- Bowling L.C., D.P. Lettenmaier, and B.V. Matheussen, 2000. "Hydroclimatology of the Arctic Drainage Basin," pp. 57-90 in L. Lewis, ed., *Freshwater Budget of the Arctic Ocean*, Kluwer, Dordrecht.
- Bradley, R.S., H.F. Diaz, J.K. Eischeid, P.D. Jones, P.M. Kelly, and C.M. Goodess. 1987. Precipitation fluctuations over Northern Hemisphere land areas since the mid-19th Century. *Science*, 237, 171-275.
- Brklacich, M., C. Bryant, B. Veenhof and A. Beauchesne, Implications of Global Climatic Change for Canadian Agriculture: A Review and Appraisal of Research from 1984 to 1997, Chapter 4 *Canada Country Study: Climate Impacts and Adaptations*. Environment Ca
- Brown, R.D. and R.O. Braaten, 1998. Spatial and temporal variability of Canadian monthly snow depths, 1946-1995. *Atmosphere-Ocean*, 36, 37-45.
- Brown, R.D., 2000. Northern Hemisphere snow cover variability and change, 1915-1997. *J. Climate*, 13, 2339-2355.
- Bubier, J.L., P.M. Crill, T.R. Moore, K. Savage, and R.K. Varner, 1998. Seasonal patterns and controls on net ecosystem CO₂ exchange in a boreal peatland complex, *Global Biogeochem. Cycles* 12: 703-714.

- Bubier, J.L., T.R. Moore, L. Bellisario, N.T. Comer and P.M. Crill, 1995. Ecological controls on methane emissions from a northern peatland complex in the zone of discontinuous permafrost, Manitoba, Canada, *Global Biogeochem. Cycles*. 9: 455-470.
- Chanton JP, Dacey JWH. 1991. Effects of vegetation on methane flux, reservoirs and carbon isotopic composition. In: Sharkey TD, Holland EA, Mooney HA (eds.) *Trace Gas Emissions from Plants*. pp. 65-92, Academic Press, San Diego CA.
- Chapin III, F. S., Shaver, G. R., Giblin, A. E., Nadelhoffer, K. J., and Laundre, J. A. ,1995. Responses of arctic tundra to experimental and observed changes in climate. *Ecology* 76:649-711.
- Chapman W. L., and J. E. Walsh, 1993. Recent variations of Sea Ice and Air Temperature in High Latitudes, *Bull. Am. Meteorol. Soc.*, 74, 33-47.
- Charlson, R.,1997. Direct climate forcing by anthropogenic sulfate aerosols: The Arrhenius paradigm a century later, *AMBIO*, Vol 26, Iss 1, pp 25-31
- Chen, J.M., Chen, W.J., Liu, J., Cihlar, J., Gray, S., 2000. Annual carbon balance of Canada's forest during 1895-1996. *Global Biogeochemical Cycles* 14:839-850.
- Cienciala, E., J. Kucera, A. and Lindroth, 1999. Long-term measurements of stand water uptake in Swedish boreal forest, *Agricultural And Forest Meteorology* (98-99)1-4, 547-554
- Cienciala, E., Kucera, J., Lindroth, A., Cermak, J., Grelle, A. & Halldin, S., 1997. Canopy transpiration from a boreal forest in Sweden during a dry year. *Agricultural and Forest Meteorology*, 86, 157-167.
- Cienciala, E., Kucera, J., Ryan, M.G. and Lindroth, A., 1998. Water flux in a forest during two hydrologically contrasting years species specific regulation of canopy conductance and transpiration. *Annales des Sciences Forestières* 55, 47-61.
- Crill PM, Harriss RC, Bartlett KB. 1991. Methane fluxes from terrestrial wetland environments. In Rogers JE, Whitman WB (eds.) *Microbial Production and Consumption of Greenhouse Gases: Methane, Nitrogen Oxides, and Halomethanes*. pp. 91-110. *Am. Soc. Micro*
- Dai et al. 1997. *Journal of Climate*.
- Dang, Q.-L., H.A. Margolis, M. Sy, M.R. Coyea, G.J. Collatz, and C.L. Walthall, 1997. Profiles of PAR, nitrogen and photosynthetic capacity in the boreal forest: implications for scaling from leaf to canopy, *J. Geophysical Research*, 102:28845-28860.
- Deardorff, J. W., 1978. Efficient Prediction of Ground Surface Temperature and Moisture, with Inclusion of a Layer of Vegetation', *J. Geophys. Res.* 83 C4, 1889-1903.
- DeFries, R.S., and J.R.G. Townshend, 1994. NDVI-derived land cover classifications at a global scale, *Int. J. Remote Sens.*, 15, 3567-3586.
- Denning, A. S., I. Fung, and D. A. Randall, 1995. Strong simulated meridional gradient of atmospheric CO₂ due to seasonal exchange with the terrestrial biota, *Nature*, 376, 240-243.
- Dewey, K.F. and R. Heim, Jr, 1982. A digital archive of Northern Hemisphere snow cover, November 1966 through December 1980. *Bull. Amer. Met. Soc.*, 63, 1132-1141.
- Ebbesmeyer, C.C., D.R. Cayan, D.R. McLain, F.H. Nichols, D.H. Peterson and K.T. Redmond. 1991. 1976 step in the Pacific climate: forty environmental changes between 1968-1975 and 1977-1984. *Proc. Seventh Annual Pacific Climate (PACLIM) Workshop, Pacific*
- Ecological Stratification Working Group, 1996. *A National Ecological Framework for Canada*. Agriculture Canada and Agri-Food Canada, Ottawa, 125 pp.
- Facchini MC; Mircea M; Fuzzi S; Charlson RJ, 1999. Cloud albedo enhancement by surface-active organic solutes in growing droplets, *NATURE*, Vol 401, Iss 6750, pp 257-259
- Fan S, Gloor M, Mahlman J, Pacala S, Sarmiento J, Takahashi T, Tans P., 1998. A large terrestrial carbon sink in North America implied by atmospheric and oceanic carbon dioxide data and models. *Nature*. 282:442-446.
- Foster, J.L., A.T.C. Chang, D.K. Hall, and A. Rango, 1991. Derivation of snow water equivalent in boreal forests using microwave radiometry. *Arctic*, 44(supplement 1), 147-152.
- Frolking S, Bubier JL, Moore TR, Ball T, Bellisario LM, Bhardwaj A, Carroll P, Crill PM, Lafleur PM, McCaughey JH, Roulet NT, Suyker AE, Verma SB, Waddington MJ, Whiting GJ, 1998. Relationship

between ecosystem productivity and photosynthetically-active r

- Frolking, S., 1997. Sensitivity of spruce/moss boreal forest net ecosystem productivity to seasonal anomalies in weather, *J. Geophysical Research*, 102:29053-29064.
- Fyfe, J.C., and G.M. Flato, 1999. Enhanced climate change and its detection over the Rocky Mountains. *J. Climate*, 12, 230-243.
- Goodison, B.E. and A.E. Walker, 1993. Use of snow cover derived from satellite passive microwave data as an indicator of climate change. *Annals of Glaciology*, 17, 137-142.
- Gorham E., 1991. Northern peatlands: role in the carbon cycle and probable responses to climatic warming. *Ecol. Appl.* 1:182-195.
- Gottschalk, L., Batchvarova, E., Gryning, S. E., Lindroth, A., Melas, D., Motovilov, Y., Fresh, M., Heikinheimo, M., Samuelsson, P., Grelle, A. and Persson, T., 1999. 'Scale aggregation - comparison of flux estimates from NOPEX', *Agric. For. Meteorol.* 98-9
- Goulden M.L., Munger J.W., Fan S-M, Daube BC, Wofsy S.C., 1996. Measurements of carbon sequestration by long-term eddy covariance: Methods and a critical evaluation of accuracy. *Global Change Biol.* 2:169-182.
- Goulden, M. L., S. C. Wofsy, J. W. Harden, S. E. Trumbore, P. M. Crill, S. T. Gower, T. Fries, B. C. Daube, S. - M. Fan, D. J. Sutton, A. Bazzaz, and J. W. Munger, 1998. Sensitivity of boreal forest carbon balance to soil thaw, *Science*, 279, 214-217.
- Goulden, M.L. and P.M. Crill., 1997. Automated measurements of CO₂ exchange at the moss surface of a black spruce forest, *Tree Physiol.*, 17: 537-542.
- Goulden, M.L., B.C. Daube, S.-M. Fan, D.J. Sutton, A. Bazzaz, J.W. Munger, and S.C. Wofsy, 1997. Physiological responses of a black spruce forest to weather, *J. Geophysical Research*, 102: 28987-28996.
- Gower, S. T., J. G. Vogel, J. M. Norman, C. J. Kucharik, S. J. Steele, and T. K. Stow, 1997. Carbon distribution and aboveground net primary production in aspen, jack pine, and black spruce stands in Saskatchewan and Manitoba, Canada. *J. Geophysical Re*
- Grelle, A. and Lindroth, A., 1994. Flow distortion by a Solent sonic anemometer: wind tunnel calibration and its assessment for flux measurements over forest and field. *J. Atmos. Oceanic Tech.* 11, 1529-1542.
- Grelle, A. and Lindroth, A., 1996. Eddy-correlation system for long-term monitoring of fluxes of heat, water vapour and CO₂. *Global Change Biology* 2, 297-307.
- Grelle, A., A. Lindroth, and M. Mölder, 1999. Seasonal variation of boreal forest surface conductance and evaporation, *Agricultural and Forest Meteorology* (98-99)1-4, 563-578
- Groisman, P. Ya, and D. Easterling, 1994. Variability and trends of total precipitation and snowfall over the United States and Canada. *J. Climate*, 7, 184-205.
- Groisman, P. Ya, T. R. Karl and R.W. Knight, 1994. Observed impact of snow cover on the heat balance and the rise of continental spring temperatures. *Science*, 263, 198-200.
- Gryning, S. E., Batchvarova, E. and De Bruin, H. A. R., 2000, 'Energy Balance of Sparse Coniferous High-Latitude Forest under Winter Conditions', *Boundary-Layer Meteorol.*, submitted.
- Gryning, S.-E. and Batchvarova, E., 1999. Regional heat flux over the NOPEX area estimated from the evolution of the mixed layer, *Agricultural and Forest Meteorology*, 98-99, 159-168.
- Gutzler, D. S., and R. D. Rosen, 1992. Interannual variability of wintertime snow cover across the Northern Hemisphere. *J. Climate*, 5, 1441-1447.
- Hall, F.G., 1999. BOREAS in 1999: Experiment and Science Overview, *Journal of Geophysical Research, Atm*, 104, D2, pp 27627-27639.
- Hall, F.G., D. Knapp and K.F. Huemmerich, "Physically based classification and satellite mapping of biophysical characteristics in the southern boreal forest." *J. Geophys. Res.*, BOREAS Special Issue, v. 102, n. 24, pp.29567, 1997.
- Halldin, S., S-E. Gryning, L. Gottschalk, A. Jochum, L-C. Lundin, A.A. Van de Griend, 1999. Energy, water and carbon exchange in a boreal forest landscape --- NOPEX experiences, *Agricultural and Forest Meteorology* (98-99)1-4, pp. 5-29

- Harden J. W., E. Sundquist, R. Stallard, and R. Mark, 1992. Dynamics of soil carbon during deglaciation of the Laurentide ice sheet, *Science*, 258, 1921-1924.
- Harden, J. W., K. P. O'Neill, S. E. Trumbore, H. Veldhuis, and B.J. Stocks, 1997. Moss and soil contributions to the annual net carbon flux of a maturing boreal forest. *J. Geophys. Res.* 102:28,805-28,816.
- Harding, R.J. and J.W. Pomeroy, 1996. The energy balance of the winter boreal landscape. *J. Climate*, 9, 2778-2787.
- Heimann M, Kaminski T, 1999. Inverse modelling approaches to infer surface trace gas fluxes from observed atmospheric mixing ratios. Pp. 277-295 in Bouwman AF (ed.) *Approaches to Scaling of Trace Gas Fluxes in Ecosystems*. Elsevier, Amsterdam.
- Hogg, E.H. and P.A. Hurdle, 1997. Sap flow in aspen: implications for stomatal responses to vapor pressure deficit, *Tree Physiology* 17:501-509.
- Hogg, E.H., T.A. Black, G. den Hartog, H.H. Neumann, R. Zimmermann, P.A. Hurdle, P.D. Blanken, Z. Nestic, P.C. Yang, R.M. Staebler, K.C. McDonald, and R. Oren, 1997. A Comparison of sap flow and eddy fluxes of water vapour from a boreal deciduous forest,
- Hogg, E.H., 1999. Simulation of interannual response of trembling aspen stands to climate variation and insects defoliation in western Canada, *Eco. Modell.* 114:175-193.
- Houghton, J.T., et al, (eds), 1995. *Climate change, science of climate change, technical summary* pp 9-97, Cambridge Univ. Press, New York.
- Jarvis, P. G. and K. G. McNaughton, 1986. Stomatal control of transpiration. *Adv. Ecol. Res.*, 15, 1-49.
- Jarvis, P. G., J. M. Massheder, S. E. Hale, J. B. Moncrieff, M. Rayment and S. L. Scott, 1997. Seasonal variation of carbon dioxide, water vapor, and energy exchanges of a boreal black spruce forest. *J. Geophys. Res.*, 102, 28953-28966.
- Joiner, D. W., J. H. McCaughey, P. M. Lafleur and P.A. Bartlett, 1999b. Water and carbon dioxide exchange at a boreal young jack pine site in the BOREAS northern study area. *J. Geophys. Res.*, 104, 27641-27652.
- Jones, P.D. 1994. Hemispheric surface air temperature variations: a reanalysis and an update to 1993. *J. Climate*, 7, 1794-1802.
- Karl, T.R., P.Y. Groisman, R.W. Knight and R.R. Heim Jr., 1993. Recent variations of snow cover and snowfall in North America and their relation to precipitation and temperature variations. *J. Climate*, 6, 1327-1344.
- Keeling, C. D., J. F. S. Chin, and T. P. Whorf, 1996. Increased activity of northern vegetation inferred from atmospheric CO₂ measurements, *Nature*, 382, 146-149.
- Kimball JS, Running SW, Saatchi SS., 1999. Sensitivity of boreal forest regional water flux and net primary production simulations to sub-grid-scale land cover complexity. *J. Geophysical Research*, 104:27789-27802.
- Koster, R. G. and M. J. Suarez, 1992. Modeling the land-surface boundary condition in climate models as a composite of independent vegetation stands. *J. Geophys. Res.*, 97, 2697-2715.
- Kurz, W.A., Apps, M.J., Bekema, S.J., Lekstrum, T., 1995. 20th century carbon budget of Canadian forests. *Tellus*, 47: 170-177.
- Lafleur, P. M., J. H. McCaughey, D.W. Joiner, P.A. Bartlett, and D.E. Jelinski, 1997. Seasonal trends in energy, water and carbon dioxide fluxes at a northern boreal wetland. *J. Geophys. Res.*, 102, 29 009-29 020.
- Larsen, J.A., *The Boreal Ecosystem*, 1980. Academic Press, New York.
- Lavigne, M.B., M.G. Ryan, D.E. Anderson, D.D. Baldocchi, P.M. Crill, D.R. Fitzjarrald, M.L. Goulden, S.T. Gower, J.M. Massheder, J.H. McCaughey, M. Rayment, and R.G. Striegl., 1997. Comparing nocturnal eddy covariance measurements to estimates of ecosystem
- Lerdau M, Litvak M, Palmer P, Monson R. 1997. Controls over monoterpene emissions from boreal forest conifers. *Tree Physiology*. 17:563-569.
- Lindroth A, Grelle A, Morén A-S, 1998. Long-term measurements of boreal forest carbon balance reveal large temperature sensitivity. *Global Change Biol.* 4:443-450.
- Lindroth, A., 1985. Canopy conductance of coniferous forests related to climate. *Water Resources Res.* 21(3): 297-304

- Liu J, Chen JM, Cihlar J, Chen W. 1999., Net primary production distribution in the BOREAS region from a process model using satellite and surface data. *J. Geophysical Research*, 104:27735-27754.
- Margolis, H.A. and M.G. Ryan, 1997. A physiological basis for biosphere-atmosphere interactions in the boreal forest: an overview, *Tree Phys.* 17: 491-499.
- McCaughey, J.H., P.M. Lafleur, D.W. Joiner, P.A. Bartlett, A.M. Costello, D.E. Jelinsky, and M.G. Ryan, 1997: Magnitudes and seasonal patterns of energy, water and carbon exchanges at a boreal young jack pine site in the BOREAS northern study area. *J. Ge*
- Melas, D., Persson, T., DeBruin, H.A.R., Gryning, S.E., Batchvarova, E., Zerefos, Submitted. Numerical Model Simulations of Boundary-Layer Dynamics during Winter Conditions:. Submitted to TAC (to the WIN-TEX/LAPP Special Issue of Theoretical and Applied Cl
- Mills, P.F., 1994. The agricultural potential of northwestern Canada and Alaska and the impact of climatic change. *Arctic* 47:115-123.
- Mitchell, J.F.B., 1983. The seasonal response of a general circulation model to changes in CO₂ and sea temperature. *Q.J.R. Meteorol. Soc.*, 109, 113-152.
- Moore T.R., Roulet N.T. ,1993. Methane flux: Water table realtions in northern wetlands. *Geophys. Res. Lett.* 20:587-590.
- Moore, T. and M. Dalva., 1993. Influence of temperature and water table position on carbon dioxide and methane emissions from columns of peatland soils. *J. Soil Sci.* 44: 651-664.
- Moosavi, S.C., and P.M. Crill., 1997. Controls on CH₄ and CO₂ emissions along two moisture gradients in the Canadian boreal zone, *J. Geophysical Research*, 102:29261-29278.
- Morén, A-S., 1999. Modelling branch conductance of Norway spruce and Scots pine in relation to climate, *Agricultural and Forest Meteorology* (98-99)1-4, 579-593
- MP Clark, MC Serreze, DA Robinson, 1999. Atmospheric controls on Eurasian snow extent. *International Journal of Climatology*, 19, 27-40.
- MSC, 2000. Canadian Snow Data CD-ROM. CRYSYS Project, Climate Processes and Earth Observation Division, Meteorological Service of Canada, Downsview, Ontario, January.
- Myneni, R. B., C. D. Keeling, C. J. Tucker, G. Asrar, and R. R. Nemani, 1997. Increased plant growth in the northern high latitudes from 1981 to 1991, *Nature*, 386, 698-702.
- Nijssen B. , G.M. O'Donnell, A.F. Hamlet, and D.P. Lettenmaier, 2000. "Hydrologic Sensitivity of Global Rivers to Climate Change," *Climatic Change*.
- NSIDC, 1999. Historical Soviet daily snow depth data - Version 2.0. National Snow and Ice Data Center, Cooperative Institute for Research in Environmental Sciences, University of Colorado, Boulder, CO. CD-ROM data product.
- Oechel, W. C. and Vourlitis, G. L., 1994. The effects of climate change on land-atmosphere feedbacks in arctic tundra regions. *Tree* 9:324-329.
- Plöchl, M. and Cramer, W. P., 1995. Coupling global models of vegetation structure and ecosystem processes - an example from Arctic and boreal ecosystems. *Tellus* 47B:240-250.
- Price, A. G., K. Dunham, T. Carleton and L. Band, 1997. Variability of water fluxes through the black spruce (*Picea mariana*) canopy and feather moss (*Pleurozium schreberi*) carpet in the boreal forest of Northern Manitoba. *J. Hydrol.*, 196, 310-323.
- Ramsay, B.H., 1998. The interactive multisensor snow and ice mapping system. *Hydrological Processes*, 12, 1537-1546.
- Randerson J.T., M.V. Thompson, T.J. Conway, I. Fung and C. Field, 1997. The contribution of terrestrial sources and sinks to trends in the seasonal cycle of atmospheric carbon dioxide, *Global Biogeochem. Cycles*, 11, 4, pp 535-560.
- Rapalee, G., S. Trumbore, E. Davidson, J. Harden, H. Veldhuis, 1998. Soil carbon stocks and their rates of accumulation and loss in a boreal forest landscape. *Global Biogeochem. Cycles*. 12:687-702.
- Rayment, M.B. and P.G. Jarvis, 1999. An improved open chamber system for measuring soil CO₂ effluxes in the field, *J. Geophys. Res.* 102, pp28,779-28,784.

- Reeburgh WS, King JY, Regli SK, Kling GW, Auerbach NA, Walker DA. 1998. A CH₄ emission estimate for the Kuparuk River basin, Alaska. *J. Geophys. Res.* 103:29005-29013.
- Reich PB, Walters MB, Ellsworth DS. 1997. From tropics to tundra: Global convergence in plant functioning. *Proc. Natl. Acad. Sci. USA.* 94:13730-13734.
- Robinson, D., and K.F. Dewey, 1990. Recent secular variations in the extent of Northern Hemisphere snow cover. *Geophys. Res. Letters*, 17, 1557-1560.
- Robinson, D.A., K.F. Dewey and R.R. Heim, 1993. Global snow cover monitoring: an update. *Bull. Am. Meteorol. Soc.*, 74, 1689-1696.
- Rosenfeld D, 1999. TRMM observed first direct evidence of smoke from forest fires inhibiting rainfall, *GEO-PHYSICAL RESEARCH LETTERS*, Vol 26, Iss 20, pp,3105-3108
- Rosenfeld D, 2000. Suppression of rain and snow by urban and industrial air pollution, *SCIENCE* , Vol 287, Iss 5459, pp 1793-1796
- Rosenfeld D., 1998. Satellite-Based Insights into Precipitation Formation Processes in Continental and Maritime Convective Clouds, *BULLETIN OF THE AMERICAN METEOROLOGICAL SOCIETY*, Vol 79, Iss 11, pp 2457-2476
- Roulet N.T., Jano A., Kelly C.A., Klinger L.F., Moore T.R., Protz R., Ritter J.A., Rouse W.R., 1994. Role of the Hudson Bay lowland as a source of atmospheric methane. *J. Geophys. Res.* 99:1439-1454.
- Roulet, N.T., P.M. Crill, N.T. Comer, A.E. Dove, and R.A. Bourbonniere, 1997. CO₂ and CH₄ between a boreal beaver pond and the atmosphere, *J. Geophysical Research*, 102:29313-29320.
- Rowe, J. S., 1972. Forest regions of Canada. Canadian Forestry Service Publication no.1300. Information Canada, Ottawa. 172 pp.
- Ruess, RW, Van Cleve K, Yarie J, Viereck LA. 1996. Comparative estimates of fine root production in successional taiga forests of interior Alaska. *Can. J. For. Res.* 26:1326-1336.
- Ryan, M.G., M.B. Lavigne, and S.T. Gower, 1997. Annual carbon costs of autotrophic respiration in boreal forest ecosystems in relation to species and climate, *J. Geophysical Research*, 102: 28871-28884.
- Saarinen, T., 1996. Biomass and production of two vascular plants in a boreal mesotrophic fen, *Can. J. Bot.* 74: 934-938.
- Savage, K., T.R. Moore, and P.M. Crill., 1997. Methane and carbon dioxide exchange between the atmosphere and northern boreal forest soils, *J. Geophysical Research*, 102: 29279-29288.
- Schlesinger M.E., and J.F.B. Mitchell, 1987. Climate model calculations of the equilibrium climatic response to increased carbon dioxide, *Reviews of Geophysics*, 25(4), 760-798.
- Schlesinger W.H., 1991. Biogeochemistry: An analysis of global change, Academic Press, San Diego Ca.
- Scialdone, J., and A. Robock, 1987. Comparison of Northern Hemisphere snow cover data sets. *J. Clim. Appl. Met.*, 26, 53-68.
- Sellers, P. J., F. G. Hall, R. D. Kelly, A. Black, D. Baldocchi, J. Berry, M. Ryan, K. J. Ranson, P. M. Crill, D. P. Lettenmaier, H. Margolis, J. Cihlar, J. Newcomer, D. Fitzjarrald, P. G. Jarvis, S. T. Gower, D. Halliwell, D. Williams, B. Goodison, D. E.
- Sellers, P. J., L. Bounoua, G. J. Collatz, D. A. Randall, D. A. Dazlich, S. O. Los, J. A. Berry, I. Fung, C. J. Tucker, C. B. Field, T. G. Jensen, 1996. Comparison of Radiative and Physiological Effects of doubled Atmospheric CO₂ Climate, *Science*, 271, 14
- Sellers, P.J., B.W. Meeson, J. Closs, J. Collatz, F. Corprew. D. Dazlich, F.G. Hall et al., 1996. The ISLSCP Initiative I global datasets: Surface boundary conditions and atmospheric forcings for land-atmosphere studies. *Bulletin American Meteorological*
- Serreze, M.C., J.E. Walsh, F.S. Chapin, T. Osterkamp, M. Dyrgerov, V. Romanovsky, W.C. Oechel, J. Morison, T. Zhang, and R.G. Barry, 2000. Observational evidence of recent change in the northern high-latitude environment. *Climatic Change*, 2000, 46, 159-2
- Silvola, J. J. Alm, U. Ahlholm, H. Nykanen, and P.J. Martikainen., 1996. CO₂ fluxes from peat in boreal mires under varying temperature and moisture conditions. *J. Ecol.* 84: 219-228.

- Simpson, I.J., G.C. Edwards, G.W. Thurtell, G. den Hartog, H.H. Neumann, and R.M. Staebler, 1997. Micrometeorological measurements of methane and nitrous oxide exchange above a boreal aspen forest, *J. Geophysical Research*, 102: 29331-29342.
- Singh, B., 1988. *The Implications of Climate Change for Natural Resources in Quebec*. Climate Change Digest Series CCD88-08. Atmospheric Environment Service, Downsview, Ontario, 11pp.
- Singh, T. and Wheaton, E. E., 1991. Boreal forest sensitivity to global warming: implications for forest management in western interior Canada. *Forestry Chronicle* 67:342-348.
- Solomon, A M and West, D C., 1987. Simulating forest ecosystem responses to expected climate change in eastern North America: applications to decision making in the forest industry, in *The Greenhouse Effect, Climate Change, and the U.S. Forests*, Shands, W
- Steele S, Gower ST, Vogel JG, Norman JM, 1997. Root mass, net primary production and turnover in aspen, jack pine and black spruce forests in Saskatchewan and Manitoba, Canada. *Tree Physiology*. 17:577-588.
- Steyaert, L.T., F.G. Hall, and T.R. Loveland, 1997. Land cover mapping, fire-regeneration, and scaling studies in the Canadian boreal forest with 1-KM AVHRR and Landsat TM Data, *J. Geophysical Research*, 102:29581-29598.
- Suffling, R., 1995. Can disturbance determining vegetation distribution during climate warming? A boreal test, *J. Biogeogra.*, 22:501-508.
- Suyker, A.E., S.B. Verma, and T.J. Arkebauer, 1997. Season-long measurement of carbon dioxide exchange in a boreal fen, *J. Geophys. Res.*, 102:29021-29028.
- Tarnocai, C., I.M. Kettles and B. Lacelle. Peatlands of Canada, 2000. Geological Survey of Canada, Open File 3834 (1:6500000 map and Digital Data Base of Canadian Peatlands)
- Thompson, D.W. J., and J.M. Wallace, 1998. The Arctic Oscillation signature in the wintertime geopotential height and temperature fields. *Geophys. Res. Lett.*, 25, 1297-1300.
- Thormann MN, Bayley S.E., 1997. Above-ground net primary production along a bog-fen-marsh gradient in southern boreal Alberta, Canada. *Écoscience* 4:374-384.
- Trumbore S.E., Bubier J.L., Harden JW, Crill P.M., 1999. Carbon cycling in boreal wetlands: A comparison of three approaches. *J. Geophys. Res.* 104:27673-27682.
- Valentini R, Matteucci H, Dolman AJ, Schulze E-D, Rebmann C, Moors EJ, Granier A, Gross P, Jensen NO, Pilegarrd K, Lindroth A, Grelle A, Bernhofer C, Grünwald T, Aubinet M, Ceulemans R, Kowalski AS, Vesala T, Rannik U, Berbigier P, Loustau D, Gudmundsson
- Van den Hurk, B.J.J.M., P. Viterbo, A.C.M. Beljaars and A. K. Betts, 2000. Offline validation of the ERA40 surface scheme. ECMWF Tech Memo, # 295, available from ECMWF, Shinfield Park, Reading RG2 9AX, UK. 43pp.
- Venäläinen, A, M. Frech, M. Heikinheimo, A. Grelle, 1999. Comparison of latent and sensible heat fluxes over boreal lakes with concurrent fluxes over a forest: implications for regional averaging, *Agricultural And Forest Meteorology* (98-99)1-4, pp. 535-54
- Vinnikov, K.Ya., P.Ya. Groisman, and K.M. Lugina, 1990. Empirical data on contemporary global climate changes (temperature and precipitation). *J. Climate*, 3, 662-677.
- Viterbo, P. and A.K. Betts, 1999. The impact on ECMWF forecasts of changes to the albedo of the boreal forests in the presence of snow. *J. Geophys. Res.*, 104, 27 803-27 810.
- Viterbo, P., A.C.M. Beljaars, J-F Mahfouf, and J. Teixeira, 1997. The representation of soil moisture freezing and its impact on the stable boundary layer. *Quart. J. Roy. Meteor. Soc.*, 125, 2401-2426.
- Weber, M.G., and M.D. Flannigan, 1997. Canadian boreal forest ecosystem structure and function in a changing climate: impact on fire regimes, *Environ. Rev.*, 5, 145-166.
- Whiting, G.J. and J.P. Chanton, 1993. Primary production control of methane emission from wetlands. *Nature* 364:794-795.
- Whittaker, R.H., and G.E. Likins, 1975. *Primary Production of the Biosphere*, Springer-Verlag, New York.
- Wiesnet, D.R., C.F. Ropelewski, G.J. Kukla, and D.A. Robinson, 1987. A discussion of the accuracy of NOAA satellite-derived global seasonal snow cover measurements. *Proc. Symp. on Large Scale Effects of Seasonal*

Snow Cover, Vancouver, Canada, IAHS, 291-30

Winston, G.C., E.T. Sunquist, B.B. Stephens, and S.E. Trumbore, 1997. Winter CO₂ fluxes in a boreal forest, *J. Geophys. Res.*, 102:28795-28804.

Wofsy SC, Goulden, M.L., J.W. Munger, S.-M. Fan, P.S. Bakwin, B.C. Daube, S.L. Bassow, and F.A. Bazzaz, 1993. Net exchange of CO₂ in a mid-latitude forest. *Science*. 260:1314-1317.

Ye, H., H-R Cho and P.E. Gustafson, 1998. The changes in Russian winter snow accumulation during 1936-83 and its spatial patterns. *J. Climate*, 11, 856-863.

Zhang, X., L.A. Vincent, W.D. Hogg and A. Nitsoo, (in press). Temperature and precipitation trends in Canada during the 20th Century. *Atmosphere-Ocean*.